JRC Scientific and Technical Reports

JRC Ispra EMEP – GAW regional station for atmospheric research

2007 report

Carsten Gruening, Mariana Adam, Francesca Barnaba, Fabrizia Cavalli, Paolo Cavalli,

Alessandro Dell'Acqua, Sebastiao Martins Dos Santos, Valerio Pagliari,

David Roux, Jean-Philippe Putaud

The mission of the Institute for Environment and Sustainability is to provide scientific-technical support to the European Union's Policies for the protection and sustainable development of the European and global environment.

***Europe Direct is a service to help you find answers
to your questions about the European Union***

Freephone number (*):

00 800 6 7 8 9 10 11

(*) Certain mobile telephone operators do not allow access to 00 800 numbers or these calls may be billed.

A great deal of additional information on the European Union is available on the Internet.
It can be accessed through the Europa server http://europa.eu/

JRC Ispra EMEP – GAW regional station for atmospheric research

2007 report

Carsten Gruening, Mariana Adam, Francesca Barnaba, Fabrizia Cavalli, Paolo Cavalli,
Alessandro Dell'Acqua, Sebastiao Martins Dos Santos, Valerio Pagliari,
David Roux, Jean-Philippe Putaud

Institute for Environment and Sustainability

Page left intentionally blank

Introduction

Location

The JRC station for atmospheric research (45°48.881'N, 8°38.165'E, 209 m asl) is located by the Northern fence of the JRC-Ispra site (Fig. 1), situated in a semi-rural area at the NW edge of the Po valley. The station is several tens of km away from large emission sources like intense road traffic or big factories. The main cities around are Varese, 20 km east, Novara, 40 km south, Gallarate - Busto Arsizio, about 20 km south-east and the Milan conurbation, 60 km to the south-east. Busy roads and highways link these urban centers. Four industrial large source points (CO emissions > 1000 tons / yr) are located between 20 and 50 km E to SE of Ispra. The closest (20 km SSE) emits also > 2000 tons of NO_x per year.

Mission

The aim of the JRC-Ispra station is to monitor the concentration of pollutants in the gas phase, the particulate phase and precipitations, as well as aerosol optical parameters, which can be used for assessing the impact of European policies on air pollution and climate change. Measurements are performed in the framework of international monitoring programs like the *Co-operative program for monitoring and evaluation of the long range transmission of air pollutants in Europe (EMEP)* of the UN-ECE Convention on Long-Range Transboundary Air Pollution *(CLRTAP)* and the *Global Atmosphere Watch (GAW)* Program of the World Meteorological Organization (WMO).

The EMEP program (http://www.emep.int/)

Currently, 50 countries and the European Community have ratified the CLRTAP. Lists of participating institutions and monitoring stations (Fig. 2) can be found at:
http://www.nilu.no/projects/ccc/network/index.html.

The set-up and running of the JRC-Ispra EMEP station resulted from a proposal of the Directorate General for Environment of the European Commission in Brussels, in agreement with the Joint Research Centre, following the Council Resolution N° 81/462/EEC, article 9.

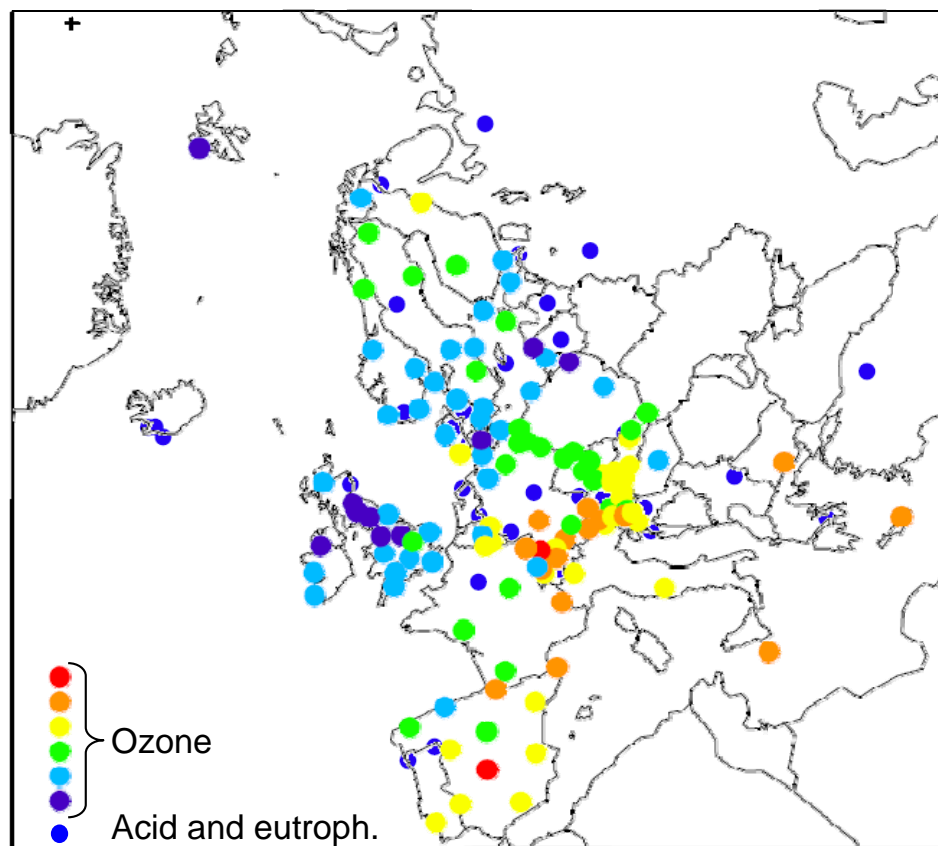*Fig. 1: location of the EMEP-GAW station inside the JRC-Ispra site*

Fig. 2: EMEP stations reporting ozone, acidifying and eutrophying data in 2005

The JRC-Ispra station operates on a regular basis in the extended EMEP measurement program since November 1985. Data are transmitted yearly to the EMEP Chemical Coordinating Centre (CCC) for data control and statistical evaluation.

The GAW program (http://www.wmo.int/web/arep/gaw/gaw_home.html)

WMO's Global Atmosphere Watch (GAW) system was established in 1989 with the scope of providing information on the physico-chemical composition of the atmosphere. These data provide a basis to improve our understanding of both atmospheric changes and atmosphere-biosphere interactions. GAW is one of WMO's most important contributions to the study of environmental issues, with about 80 member countries participating in GAW's measurement program. Since December 1999, the JRC-Ispra station is also part of the GAW coordinated network of regional stations. Aerosol data submitted to EMEP automatically flow to the GAW World Data Center for Aerosol (WDCA).

The institutional program (http://ccu.jrc.ec.europa.eu)

The JRC-Ispra station has been managed by the Climate Change Unit of the Joint Research Centre's (JRC) Institute for Environment and Sustainability since February 2002. From then on, its monitoring program has been focused on air pollution and climate forcing of short-lived agents such as tropospheric ozone and aerosols. Concretely, more sensitive gas monitors were introduced, as well as a set of new measurements providing aerosol characteristics that are linked to its radiative forcing.

The site is also being used for research and development purposes, mainly focusing on organic carbon sampling artefacts. The data obtained in Ispra are used for the design of the EMEP monitoring strategy and the revision of the EMEP sampling and analytical procedure manual.

Historical data can be downloaded from the Climate Change Unit web page by selecting "what we do" → "existing datasets" and then EMEP station data.
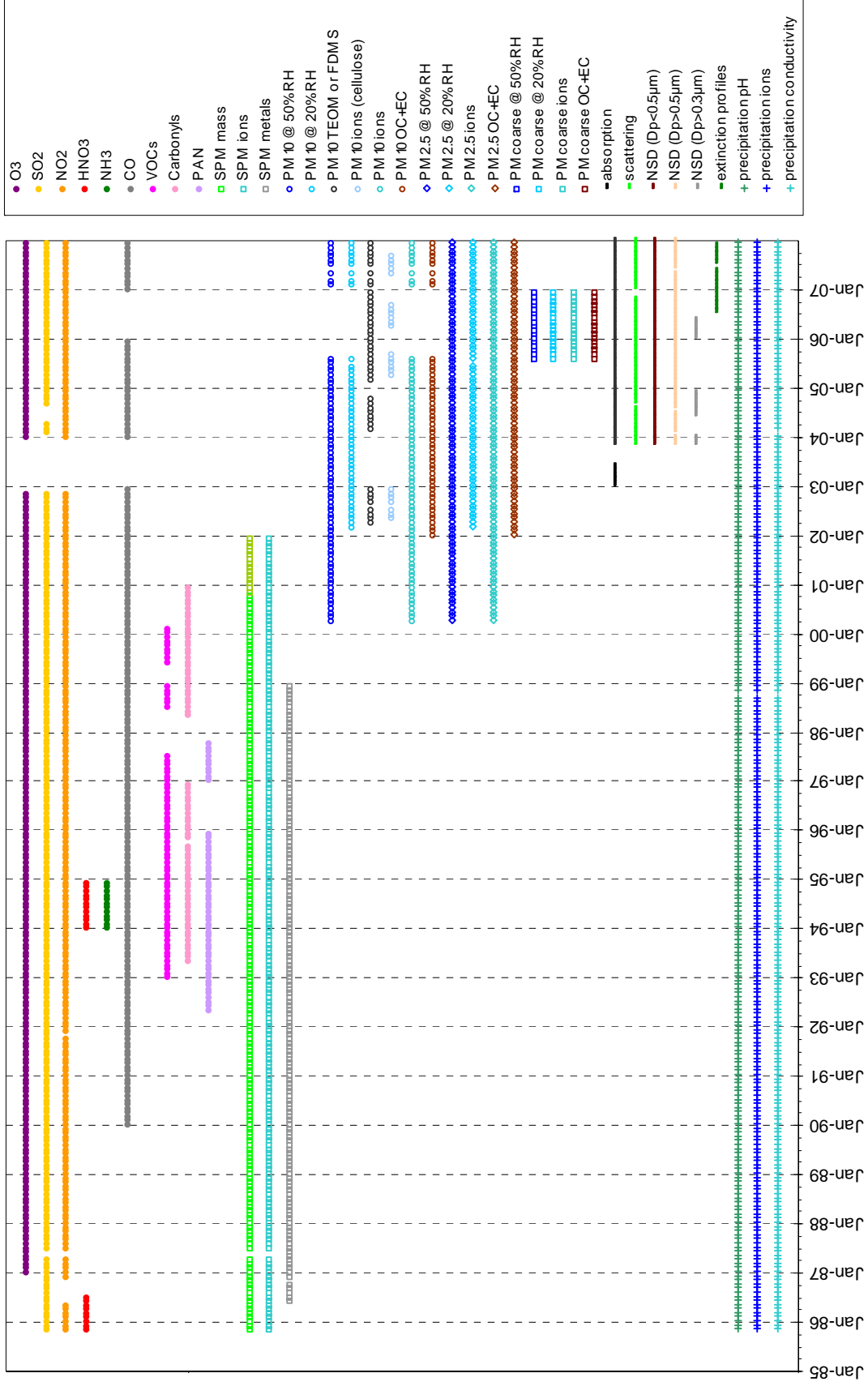
Fig. 3: measurements performed at the JRC-Ispra station for atmospheric research since 1985

The JRC-Ispra station for atmospheric research monitoring program

Since 1985, the JRC-Ispra air monitoring station program evolved significantly (Fig. 3). The parameters measured at the JRC-Ispra station in 2007 are listed in Table 1. Fig. 4 shows the data coverage for 2007.

Meteorological parameters as well as the gas phase species SO_2, NO_x, O_3 and CO were measured during the whole year 2007. CO concentrations though are not reported because of instrumental problems that could not be corrected. 24-hr integrated (from 08:00 to 08:00 UTC) particulate matter (PM2.5) samples were collected daily and analyzed for PM2.5 mass (at 20 and 50% RH), main ions, OC and EC. PM10 24-hour filter samples were normally collected four times a month on average and analyzed in the same way as the daily PM2.5 samples. On-line PM10 measurements (FDMS-TEOM) were carried out for the whole year, except for short breaks due to technical problems or maintenance. Aerosol absorption coefficient and particle number size distribution (Dp < 600 nm) were measured continuously over the whole year. Particle number size distribution (Dp > 500 nm), and scattering coefficient were determined continuously as well. The LIDAR provided altitude resolved aerosol backscattering profiles during favourable weather conditions except for longer interruptions in June / mid-July and mid-November / December due to instrumental problems. Precipitation was collected throughout the year and analyzed for pH, conductivity, and main ions.

Table 1: parameters measured during 2007

| METEOROLOGICAL PARAMETERS	pressure, temperature, humidity, wind, solar radiation
GAS PHASE	SO_2, NO, NO_2, NO_X, O_3, CO
PARTICULATE PHASE	For $PM_{2.5}$: PM mass and Cl^-, NO_3^-, SO_4^{2-}, $C_2O_4^{2-}$, Na^+, NH_4^+, K^+, Mg^{2+}, Ca^{2+}, OC, and EC
	For PM_{10}: PM mass and Cl^-, NO_3^-, SO_4^{2-}, $C_2O_4^{2-}$, Na^+, NH_4^+, K^+, Mg^{2+}, Ca^{2+}, OC, and EC
	Number size distribution (10 nm - 10 µm)
	Aerosol absorption, scattering and back-scattering coefficient
	altitude-resolved aerosol back-scattering
PRECIPITATION PHASE	Cl^-, NO_3^-, SO_4^{2-}, $C_2O_4^{2-}$, Na^+, NH_4^+, K^+, Mg^{2+}, Ca^{2+} pH, conductivity
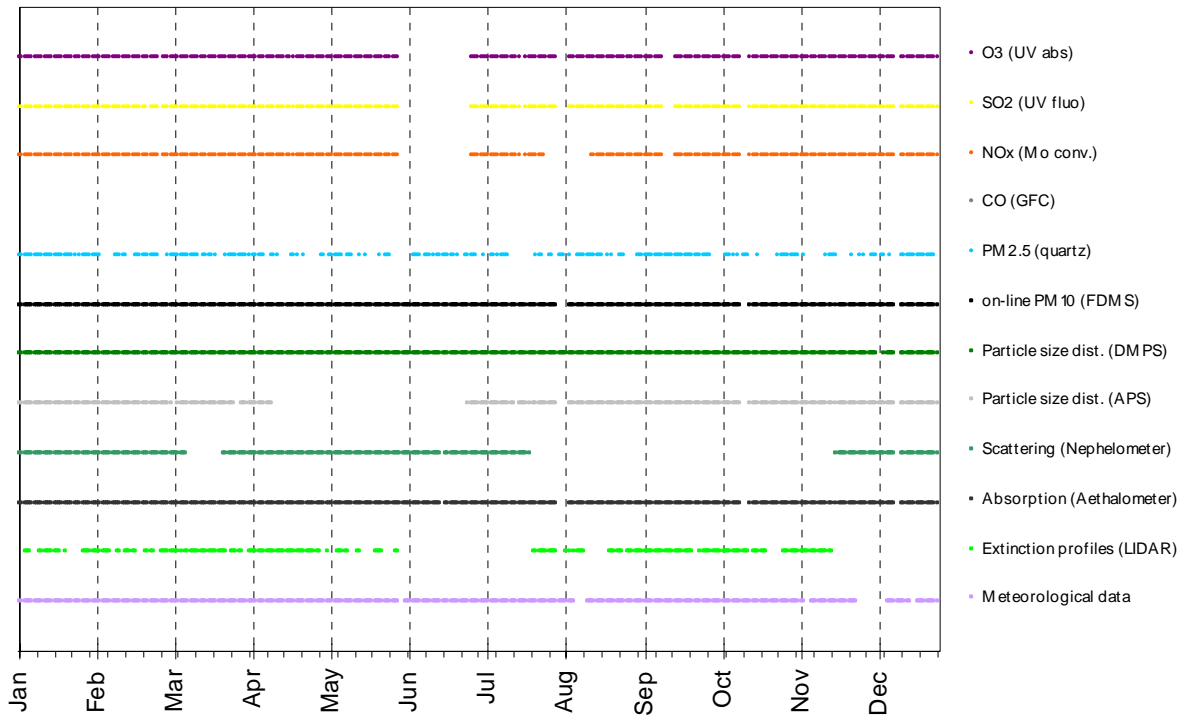
Fig. 4: 2007 data coverage

The measurement techniques

On-line Monitoring

Meteorological Parameters

Weather Transmitter:

Meteorological data and solar radiation were measured directly at the EMEP station with the instrumentation described below.

WXT510 (S/N: A1410004)

A WXT510 weather transmitter from Vaisala has been installed that records simultaneously the six weather parameters temperature, pressure, relative humidity, precipitation and wind speed and direction.
The wind data measurements utilise three equally spaced ultrasonic transducers that determine the wind speed and direction from the time it takes for ultrasound to travel from one transducer to the two others. The precipitation is measured with a piezoelectrical sensor that detects the impact of individual raindrops and thus infers the accumulated rainfall. For the pressure, temperature and humidity measurements, separate sensors employing high precision RC oscillators are used.

CM11 (S/N: 058911)

To determine the solar radiation, a Kipp and Zonen CM11 Pyranometer has been installed that measures the irradiance (in W/m^2) on a plane surface from direct solar radiation and diffuse radiation incident from the hemisphere above the device. The measurement principle is based on a thermal detector. The radiant energy is absorbed by a black disc and the heat generated flows through a thermal resistance to a heat sink. The temperature difference across the thermal resistance is then converted into a voltage and precisely measured. The CM11 features a fast response time of 12 s, a small non stability of +/-0.5 % and a small non linearity of +/-0.2 %.

Gaseous Air Pollutants

Sampling

Gases are sampled from a common inlet situated at 3.5 m above the ground on the roof of the gas monitors' container. The sampling line consists in an inlet made of a PVC semi-spherical cap (to prevent rain and bugs enter the line), a PTFE tube (Ø=2.54 cm, h=150 cm), the lower part of which is kept at 60 (±10) °C, and a "multi-channel distributor" glass tube kept at 40 (±10) °C (by internal heating), with nine 14mm lateral threaded connectors. This inlet is flushed by a 34 L/min flow (*measured with RITTEWR 11456*). Each instrument samples from the glass tube with its own pump through a ¼" Teflon line and a 1 µm pore size 47 mm diameter Teflon filter (to eliminate particles from the sampled air).

In 2007, the gas monitors were calibrated 4 times only due to a lack of suitable span gas cylinders. Sampling flow rates are as follow:

Analyte	L/min
CO	1.6
SO_2	0.5
NO, NO_2, NO_x	0.6
O_3	2.0

CO: *Non-Dispersive Infrared Gas-Filter Correlation Spectroscopy*

Thermo 48C-TL (S/N 60873-328)

A *Gas-Filter Correlation (*GFC) monitor (Burch et al., 1976) has the advantages of a NDIR instrument: no interference from CO_2, and very small interference from water vapor. During operation, air flows continuously through a sample cell. Radiation from the source is directed by optical transfer elements through two main optical subsystems: (1) the rotating gas filter and (2) the optical multi-path (sample) cell. The beam exits the sample cell through interference filter, which limits the spectral passband to a few of the strongest CO absorption lines in the 4.6-µm region. Detection of the transmitted radiation occurs with the infrared detector. The gas correlation cell is constructed with 4 compartments: 2 compartments are filled with 0.5 atm CO, and the two others are filled with pure N_2. Radiation directed to the CO compartment is completely attenuated at wavelengths where CO absorbs strongly. The radiation transmitted through the N_2 is reduced by covering the exit window of the N_2 cells with a neutral attenuator so that the amounts of radiation transmitted by the CO and N_2 cells are made approximately equal. During operation, radiation passes alternately through the two types of cells as they are rotated to establish a frequency modulated signal. If CO is present in the sample, the radiation transmitted through the CO cell is not appreciably changed, as it is already strongly absorbed in the CO cell, whereas the radiation through the N_2 cell is changed. This imbalance is linearly related to CO concentrations in ambient air.

Calibration is performed using a zero air gas cylinder (Air Liquide, CnHm<0.5 ppm) and an external span gas. The span gas cylinder (2104G, 3514B and 160420 from Messer Griesheim GmbH) concentrations (9.999 ± 0.0005, 9.999 ± 0.0005 and 8.12 ±0.07 ppm, respectively) were determined at ERLAP (European Reference Laboratory of Air Pollution) in October 2005. The instrument's lower detection limit is 0.02 ppm.

SO_2: *UV Fluorescent SO_2 Analyser*

Thermo 43C TL (S/N 0401904668)

At first, the air flow is scrubbed to eliminate aromatic hydrocarbons. The sample is then directed to a chamber where it is irradiated by 214 nm (UV), a wavelength that SO_2 molecules absorb. The fluorescence signal emitted by the excited SO_2 molecules going back to the ground state is filtered between 300 and 400 nm (specific of SO_2) and amplified by a photomultiplier tube. A microprocessor receives the electrical zero and fluorescence reaction intensity signals and calculates SO_2 based on a linear calibration curve.

Calibration is performed using a zero air gas cylinder (Air Liquide, CnHm<0.5 ppm) and external span gas cylinders 6474D (67.2 ± 2 ppb). The span gas cylinder (from Messer Griesheim GmbH) concentration were controlled at ERLAP in October 2005.

The specificity of the trace level instrument (TEI 43C-TL) is that it uses a pulsed lamp. The 43C-TL's detection limit is 0.2 ppb (ca. 0.5 µg/m³) according to the technical specifications.

NO + NO$_X$: Chemiluminescent Nitrogen Oxides Analyzer

Thermo 42C (S/N 62581-336 and S/N 0401304317)

This nitrogen oxides analyser is based on the principle that nitric oxide (NO) and ozone react to produce excited NO$_2$ molecules, which emit infra-red photons when going back to lower energy states:

$$NO + O_3 \rightarrow NO_2 + O_2 + h\nu$$

A stream of purified air (dried with a Nafion Dryer) passing through a silent discharge ozonator generates the ozone concentration needed for the chemiluminescent reaction. The specific luminescence signal intensity is therefore proportional to the NO concentration. A photomultiplier tube amplifies this signal.

NO$_2$ is detected as NO after reduction in a Mo converter heated at about 325 °C.

The ambient air sample is drawn into the analyzer, flows through a capillary, and then to a valve, which routes the sample either straight to the reaction chamber (NO detection), or through the converter and then to the reaction chamber (NO$_X$ detection). The calculated NO and NO$_X$ concentrations are stored and used to calculate NO$_2$ concentrations, assuming that only NO$_2$ is reduced in the Mo converter.

Calibration is performed using a zero air gas cylinder (Air Liquide, CnHm<0.5 ppm) and a NO span gas. The NO span gas cylinders 551C (from Messer Griesheim GmbH) concentrations (113.2 ± 0.5 ppb) were controlled in Oct. 2005 at ERLAP.

O$_3$: UV Photometric Ambient Analyzer

Thermo 49C (S/N 55912-305 and S/N 0503110499)

The UV photometer determines ozone concentrations by measuring in the absorption cell the attenuation of UV light (254 nm) due to ozone. The concentration of ozone is related to the magnitude of the attenuation. The reference gas, generated by scrubbing ambient air, passes into one of the two absorption cells to establish a zero light intensity reading, I$_0$. Then the sample passes through the other absorption cell to establish a sample light intensity reading, I. This cycle is reproduced with inverted cells. The average ratio R=I/I$_0$ between 4 consecutive readings is directly related to the ozone concentration in the air sample through the Beer-Lambert law.

Calibration is performed using externally generated zero air and external span gas. Zero air is taken from a gas cylinder (Air Liquide, CnHm < 0.5 ppm). Span gas (50 ppb in winter and 100 ppb in summer and high concentration periods) is generated by a TEI 49C-PS transportable primary standard ozone generator (S/N 0503110396) calibrated at ERLAP (European Reference Laboratory of Air Pollution) in April 2007.

The ozone monitor, together with all other gas monitors, participated during the entire month of June in an intercomparison exercise at the ERLAP. Because the summer months have the highest ozone concentrations and ozone metrics such as SOMO35 and AOT40 rely on high data coverage, ozone concentrations measured at the ARPA station at Milan-Malpensa (www.arpalombardia.it/qaria/doc_RichiestaDati.asp) have been used for June 2007.

Aerosol

PM10 mass concentration: Tapered Element Oscillating Mass balance, Series 1400a

Thermo FDMS – TEOM (S/N 140AB233870012)

The Series 1400a TEOM® monitor incorporates an inertial balance patented by Rupprecht & Patashnick. It measures the mass collected on an exchangeable filter cartridge by monitoring the frequency changes of a tapered element. The sample flow passes through the filter, where particulate matter is collected, and then continues through the hollow tapered element on its way to an electronic flow control system and vacuum pump. As

more mass collects on the exchangeable filter, the tube's natural frequency of oscillation decreases. A *direct* relationship exists between the tube's change in frequency and mass on the filter. The TEOM mass transducer does not require recalibration because it is designed and constructed from non-fatiguing materials. Calibration may be verified, however, using an optional Mass Calibration Verification Kit that contains a filter of known mass.

The instrument set-up includes a Sampling Equilibration System (SES) that allows a water strip-out without sample warm up by means of Nafion Dryers. In this way the air flow RH is reduced to < 30%, when TEOM® operates at 30 °C only. The Filter Dynamic Measurement System (FDMS) is based on measuring changes of the TEOM filter mass when sampling alternatively ambient and filtered air. The changes in the TEOM filter mass while sampling filtered air is attributed to sampling (positive or negative) artefacts, and is used to correct changes in the TEOM filter mass observed while sampling ambient air.

Particle number size distribution: Differential Mobility Particle Sizer (DMPS)

DMA "A", CPC TSI 3010 (S/N 2007), CPC TSI 3010 (S/N 2052)

The Differential Mobility Particle Sizer consists in a home-made medium size (28 cm) Vienna-type Differential Mobility Analyser (DMA) and a Condensation Particle Counter (CPC), TSI 3010 (S/N 2007) till 24.08.2007 and then TSI 3010 (S/N 2052).

DMAs use the fact that electrically charged particles move in an electric field according to their electrical mobility. Electrical mobility depends mainly on particle size and electrical charge. Atmospheric particles are brought in the bipolar charge equilibrium in the bipolar diffusion charger (TSI neutralizer till 30/8/2007, new Eckert & Ziegler neutralizer with 370 MBq afterwards): a radioactive source (Kr-85) ionizes the surrounding atmosphere into positive and negative ions. Particles carrying a high charge can discharge by capturing ions of opposite polarity. After a very short time, particles reach a charge equilibrium such that the aerosol carries the bipolar Fuchs-Boltzman charge distribution. A computer program sets stepwise the voltage between the 2 DMA's electrodes (from 10 to 11500 V). Negatively charged particles are so selected according to their mobility. After a certain waiting time, the CPC measures the number concentration for each mobility bin. The result is a particle mobility distribution. The number size distribution is calculated from the mobility distribution by an inversion routine (from A. Wiedensohler) based on the bipolar charge distribution and the size dependent DMA transfer function. The CPC detection efficiency curve is not taken into account. The DMPS measured aerosol particles in the range 10 – 600 nm. It displays data using 45 size channels (32 channels per decade) for high-resolution size information. This submicrometer particle sizer is capable of measuring concentrations in the range from 1 to 2.4×10^6 particles/cm^3. The DMPS generates a new particle size distribution every eight minutes. It is possible to set ambient pressure and temperature, so there is no need for post-acquisition data correction.

Accessories include:
- FUG High voltage cassette power supplies Series HCN7E – 12500 Volts.
- Membrane pump KNF (sampling aerosol at 1 cm³/min)
- Vacuum pump (circulating dry sheath air (<20% RH), using Silicagel, at 8.3 cc/min)
- Magnehelic for sheath air flow quick visual check

Particle number size distribution: Aerodynamic Particle Sizer

APS TSI 3321 (S/N 70535014)

The APS 3321 is a time-of-flight spectrometer that measures the velocity of particles in an accelerating air flow through a nozzle.

Ambient air is sampled at 1 L/min, sheath air (from the room) at 4 L/min. In the instrument, particles are confined to the centerline of an accelerating flow by sheath air. They then pass through two broadly focused laser beams, scattering light as they do so.

Side-scattered light is collected by an elliptical mirror that focuses the collected light onto a solid-state photodetector, which converts the light pulses to electrical pulses. By electronically timing between the peaks of the pulses, the velocity can be calculated for each individual particle.

Velocity information is stored in 1024 time-of-flight bins. Using a polystyrene latex (PSL) sphere calibration, which is stored in non-volatile memory, the APS Model 3321 converts each time-of-flight measurement to an aerodynamic particle diameter. For convenience, this particle size is binned into 52 channels (on a logarithmic scale).

The particle range spanned by the APS is from 0.5 to 20 μm in both aerodynamic size and light-scattering signal. Particles are also detected in the 0.3 to 0.5 μm range using light-scattering alone, and are binned together in one channel. The APS is also capable of storing correlated light-scattering-signal. *dN/dLogDp* data are averaged over 10 min.

Particle scattering and back-scattering coefficient

Nephelometer TSI 3563 (S/N 1081)

The integrating nephelometer is a high-sensitivity device capable of detecting the scattering properties of aerosol particles. The nephelometer detects by measuring the light scattered by the aerosol and then subtracting light scattered by the walls of the measurement chamber, light scattered by the gas, and electronic noise inherent in the detectors.

Ambient air is sampled at 20 L/min from a whole air inlet (TSP). The three-color detection version of TSI nephelometer detects scattered light intensity at three wavelengths (450, 550, and 700 nm). Normally the scattered light is integrated over an angular range of 7–170° from the forward direction, but with the addition of the backscatter shutter feature to the Nephelometer, this range can be adjusted to either 7–170° or 90–170° to give total scatter and backscatter signals. A 75 Watt quartz-halogen white lamp, with a built-in elliptical reflector, provides illumination for the aerosol. The reflector focuses the light onto one end of an optical pipe where the light is carried into the internal cavity of the instrument. The optical pipe is used to thermally isolate the lamp from the sensing volume. The output end of the optical light pipe is an opal glass diffuser that acts as a *quasi*-cosine (Lambertian) light source. Within the measuring volume, the first aperture on the detection side of the instrument limits the light integration to angles greater than 7°, measured from the horizontal at the opal glass. On the other side, a shadow plate limits the light to angles less than 170°. The measurement volume is defined by the intersection of this light with a viewing volume cone defined by the second and fourth aperture plates on the detection side of the instrument. The fourth aperture plate incorporates a lens to collimate the light scattered by aerosol particles so that it can be split into separate wavelengths. The nephelometer uses a reference chopper to calibrate scattered signals. The chopper makes a full rotation 23 times per second. The chopper consists of three separate areas labelled: signal, dark, and calibrate.

The signal section simply allows all light to pass through unaltered. The dark section is a very black background that blocks all light. This section provides a measurement of the photomultiplier tube (PMT) background noise. The third section is directly illuminated this section to provide a measure of lamp stability over time. To reduce the lamp intensity to a level that will not saturate the photomultiplier tubes, the calibrate section incorporates a neutral density filter that blocks approximately 99.9 % of the incident light. To subtract the light scattered by the gas portion of the aerosol, a high-efficiency particulate air (HEPA) filter is switched in line with the inlet for 300 s every hour. This allows compensation for changes in the background scattering of the nephelometer, and in gas composition that will affect Rayleigh scattering of air molecules with time. When the HEPA filter is not in line with the inlet, a small amount of filtered air leaks through the light trap to keep the apertures and light trap free of particles. A smaller HEPA filter allows a small amount of clean air to leak into the sensor end of the chamber between the lens and second aperture. This keeps the lens clean and confines the aerosol light scatter to the measurement volume only.

Nephelometer data are corrected for angular non idealities and truncation errors according to Anderson and Ogren, 1998. Large hygroscopic effects are expected for internal RH > 60%, which can statistically occur from May to Sept. Atmospheric particle scattering coefficients presented in this report are **not** corrected for RH effects, except when specified.

Particle absorption coefficient

Aethalometer Magee AE-31 (S/N 408: 0303)

The principle of the Aethalometer is to measure the attenuation of a beam of light transmitted through a filter, while the filter is continuously collecting an aerosol sample. Suction is provided by an internally-mounted pump. Attenuation measurements are made at successive regular intervals of a time base period. The objectives of the Aethalometer hardware and software systems are as follows:
(a) to collect the aerosol sample with as few losses as possible on a suitable filter material;
(b) to measure the optical attenuation of the collected aerosol deposit as accurately as possible;
(c) to calculate the rate of increase of the equivalent black carbon (EBC) component of the aerosol deposit and to interpret this as an EBC concentration in the air stream;
(d) to display and record the data, and to perform necessary instrument control and diagnostic functions.

The optical attenuation of the aerosol deposit on the filter is measured by detecting the intensity of light transmitted through the spot on the filter. In the AE-31, light sources emitting at different wavelengths (370, 470, 520, 590, 660, 880 and 950 nm) are also installed in the source assembly. The light shines through the lucite aerosol inlet onto the aerosol deposit spot on the filter. The filter rests on a stainless steel mesh grid, through which the pumping suction is applied. Light penetrating the diffuse mat of filter fibers can also pass through the spaces in the support mesh. This light is then detected by a photodiode placed directly underneath the filter support mesh. As the EBC content of the aerosol spot increases, the amount of light detected by the photodiode will diminish.
For highest accuracy, we must make further measurements: the amount of light penetrating the combination of filter and support mesh is relatively small, and a correction is needed for the 'dark response signal' of the overall system. This is the electronics' output when the lamps are off: typically, it may be a fraction of a percent of the response when the lamps are on. To eliminate the effect of the dark response, we take 'zero' readings of the system response with the lamps turned off, and subtract this 'zero' level from the response when the lamps are on.
The other measurement necessary for the highest accuracy is a 'reference beam' measurement to correct for any small changes in the light intensity output of the source. This is achieved by a second photodiode placed under a different portion of the filter that is not collecting the aerosol, on the left-hand side where the fresh tape enters. This area is illuminated by the same lamps. If the light intensity output of the lamps changes slightly, the response of this detector is used to mathematically correct the 'sensing' signal. The reference signal is also corrected for dark response 'zero' as described above.
The algorithm in the computer program (see below) can account for changes in the lamp intensity output by always using the ratio quantity [Sensing]/[Reference]. As the filter deposit accumulates EBC, this ratio will diminish.
In practice, the algorithm can account for lamp intensity fluctuations to first order, but we find a residual effect when operating at the highest sensitivities. To minimize this effect and to realize the full potential of the instrument, it is desirable for the lamps' light output intensity to remain as constant as possible from one cycle to the next, even though the lamps are turned on and off again. The computer program monitors the repeatability of the reference signal, and issues a warning message if the fluctuations are considered unacceptable. When operating properly, the system can achieve a reference beam

repeatability of better than 1 part in 10000 from one cycle to the next. The electronics circuit board converts the optical signals directly from small photocurrents into digital data, and passes it to the computer for calculation. A mass flow meter monitors the sampled air flow rate. These data and the result of the EBC calculation are written to disk and displayed on the front panel of the instrument.

Aethalometer data are corrected for the shadowing effect and for multiple-scattering in the filter to derive the aerosol absorption coefficient (Arnott et al., 2005) with a correction factor C = 3.65 for green light.

Range-resolved aerosol backscattering, extinction and aerosol optical thickness

Cimel Aerosol Micro Lidar (CAML) CE 370-2 (laser & electronics: S/N 0507-846 and telescope: S/N 0507- 847)

In 2006, an aerosol backscatter LIDAR instrument (LIght Detection And Ranging) has been installed at the EMEP station for the range-resolved optical remote sensing of aerosols. It serves to bridge the gap between local, in-situ measurements of aerosols at the ground and satellite based characterizations of the aerosol column above ground. To reach this, altitude resolved aerosol backscattering, aerosol extinction and the aerosol optical thickness (AOT) are derived from LIDAR data with high time resolution.

LIDAR measurements are based on the time resolved detection of the backscattered signal of a short laser pulse that is sent into the atmosphere (for an introduction see Weitkamp, C. 2005). Using the speed of light, time is converted to the altitude where the backscattering takes place. Utilising some assumptions about the atmospheric composition, **aerosol backscattering, extinction and aerosol optical thickness** can be derived using the LIDAR equation. The received power P of the detector is therein given as a function of distance and wavelength by:

$$P(R,\lambda) = P_0 \, {}^{c\tau}\!/_2 \, A\eta \, \frac{O(R)}{R^2} \beta(R,\lambda) \exp\left(-2\int_0^R \alpha(r,\lambda)dr\right)$$

Form. 1: P_0: power of the laser pulse, c: speed of light, τ: laser pulse length, A: area of the receiving optics, η: system efficiency, R: distance, O: overlap function between laser pulse and receiving optics, λ: wavelength, β: backscatter coefficient, α: absorption coefficient

LIDAR measurements were performed with a Cimel Aerosol Micro Lidar (CAML). CAML is an eye-safe, single-wavelength, monostatic aerosol backscatter lidar. The lidar emitter is a diode pumped, frequency doubled Nd:YAG laser operating at a wavelength of 532 nm, with a repetition rate of 4.7 kHz and a pulse energy of 8 μJ/pulse. The pulse width is ~ 3ns. The integration time of the detector (100ns) allows the sampling at 15m resolution Depending on the actual atmospheric conditions, the maximum vertical range for probing the atmosphere can go up to maximum 15 km.

Eye-safety of the system is reached by expanding the laser beam trough a 20 cm diameter, 1 m focal length refractive telescope. The emission and reception optical paths coincide through a single, 10 m long optical fibre that connects both the laser output and receiving detector with the telescope. The telescope field of view is approximately 50 μrad. The backscatter signal is sent to the receiver passing through a narrow bandpass interference filter (0.2 nm fwhm, centred at 532 nm) to reduce the background level. To avoid saturation of the detector immediately after the laser pulse is emitted and thus reduce the afterpulse signal, an acousto-optical modulator is placed before the detector that blocks the light from the detector that is directly backscattered from optical components in the light path. The detector is an avalanche photodiode photon-counting module with a high quantum efficiency approaching 55 % with maximum count rates near 20 MHz.

Data evaluation is done with an inversion algorithm based on an iteration-convergence method for the LIDAR equation (see Form. 1) that has been implemented in-house using the MATLAB programming environment. Starting with the CAML raw data, the 10 minutes time averages of the backscatter profiles are space–averaged over 60 m. Then the background is subtracted and the result is corrected for a so called 'afterpulse' contribution. This originates from light that is scattered back to the detector from all surfaces on the optical path to the telescope. As its intensity is rather high compared to the atmospheric backscatter, it influences the raw detector signal. From July 2007 onwards, this 'afterpulse' method has been substituted by using a linear fit to the signal at the far end for a profile specific afterpulse and background correction. Furthermore, the overlap function $O(R)$ (see Form. 1) is applied to the data before it is range corrected, i.e. multiplied by R^2. This range corrected signal constitutes the level 0 data.

Using the US standard atmosphere to calibrate the molecular backscattering in an aerosol free region and assuming a LIDAR ratio (i.e. extinction-to-backscatter ratio) that is constant with height, the aerosol backscatter, extinction and optical thickness (AOT) profiles are provided as level 1 data. The best estimates of the LIDAR ratios (LR) that have been used for the data inversion ranged from LR = 20 in winter to LR = 70 during summer.

The measurement schedule for acquiring LIDAR profiles is a compromise between good temporal coverage and extended lifetime of the laser diodes: the LIDAR runs for 10 minutes, and is switched off for 20 minutes. This 30 minute cycle is repeated continuously during favourable weather conditions, i.e. no precipitation and no cloud coverage that would absorb the laser pulse and thus prevent meaningful aerosol LIDAR measurements. LIDAR profiles of the atmosphere have been acquired during the whole year except for June and November / December when the instrument had technical problems.

Sampling and off-line analyses

<u>Particulate Matter</u>

PM2.5 from quartz fibre filters

PM2.5 was continuously sampled at 16.7 L/min on quartz fibre filters with a Partisol sampler, without charcoal stripe denuder and a PM10 + cyclone with cut @ 2.5 µm sampling head. The sampled area is 42 mm Ø in both samplers. Filters were from PALL Life Sciences (type TISSUEQUARTZ 2500QAT-UP). Filter changes occurred daily at 08:00 UTC.

Filters were weighed at 50 % (EN 12341 procedure) and 20 % RH before and after exposure with a microbalance Sartorius MC5 placed in a controlled (dried or moisture added and scrubbed) atmosphere glove box. They were stored at 4 °C until analysis.

Main ions (Cl^-, NO_3^-, SO_4^{2-}, $C_2O_4^{2-}$, Na^+, NH_4^+, K^+, Mg^{2+}, Ca^{2+}) were analysed by ion chromatography (Dionex DX 120 with electrochemical eluent suppression) after extraction of the soluble species in an aliquot of 16 mm Ø in 20 ml 18.2 MOhm cm resistivity water (Millipore mQ).

Organic and elemental carbon (OC+EC) were analysed using a Sunset Dual-optical Lab Thermal-Optical Carbon Aerosol Analyser (S/N 173-5). PM2.5 samples were analysed using the EUSAAR-1 thermal protocol that has been developed to minimize biases inherent to thermo-optical analysis of OC and EC (Cavalli 2008):

Fraction Name Sunset Lab.	Plateau Temperature (°C)	Duration (s)	Carrier Gas
OC 1	200	120	He 100%
OC 2	300	150	He 100%
OC 3	450	180	He 100%
OC 4	650	180	He 100%
cool down		30	He 100%
EC1	550	240	He:O_2 99:1
EC2	850	150	He:O_2 99:1

In addition, cellulose Whatman 40 cellulose filters were collected in the extended summer months from 5th of April till 30th of August to assess NH_4NO_3 losses that occur during higher temperatures for sampling on quartz filters.

PM10 from quartz fibre filters

PM10 was usually sampled 4 times per month for a 24 h period at 16.7 L/min on quartz fibre filters (TISSUEQUARTZ 2500QAT-UP) with a Partisol sampler using a PM10 sampling head. Filter preparation and analysis has been performed exactly as described above for PM2.5 samples to check for differences in the chemical composition of coarse particles compare to PM2.5.In total, 31 filters have been sampled and analyzed.

Wet-only deposition

For the precipitation collection, two Eigenbrodt wet-only samplers (S/N 3311 and 3312) were used that automatically collect the rainfall in a 1 L polyethylene container. The collection surface is 550 cm^2. 24-hr integrated precipitation samples (if any) are collected every day starting at 8:00 UTC.

All collected precipitation samples were stored at 4 °C until analyses (ca. every 3 months).

Analyses include the determinations of pH and conductivity at 25 °C with a Sartorius Professional Meter PP-50 and principal ion concentrations (Cl^-, NO_3^-, SO_4^{2-}, $C_2O_4^{2-}$, Na^+, NH_4^+, K^+, Mg^{2+}, Ca^{2+}) by ion chromatography (Dionex DX 120 with electrochemical eluent suppression).
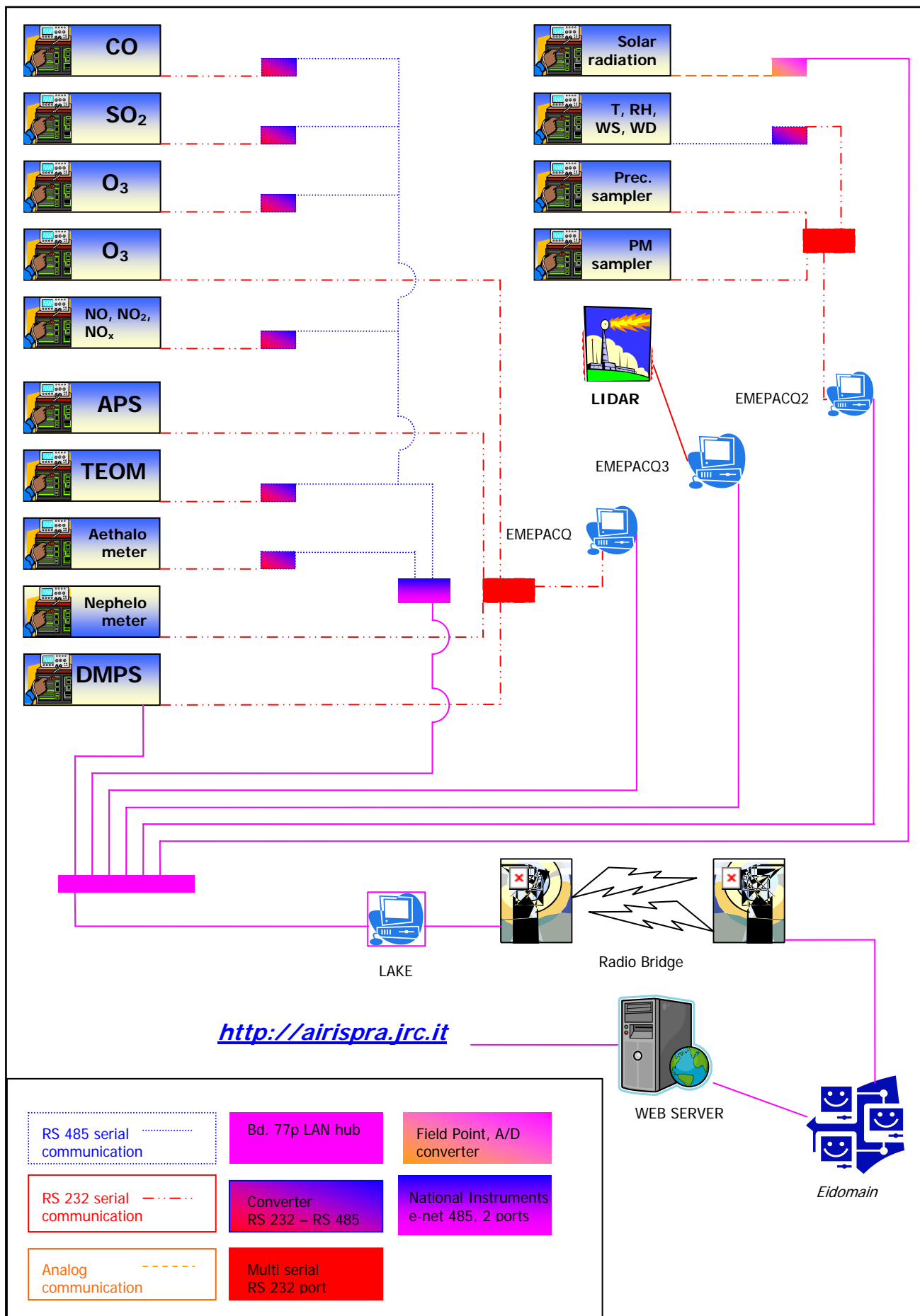
Fig. 5: setup of the EMEP GAW station Data Acquisition System

On-line data acquisition system

The JRC EMEP-GAW station Data Acquisition System (DAS) is a home made set of hardware and software, designed to operate instruments, acquire both analog and digital output from instruments and store pre-processed measurement data into a database for further off-line evaluation. The DAS operated and controlled the instrumentation during 2007, software bug fixed and updates were implemented when necessary.

The software environment of the DAS is Labview 7.1 from National Instruments and the database engine for data storage is Microsoft Access.

The DAS is designed to continuously run the following tasks:

- Start of the data acquisition at a defined time (must be full hour);
- Choose the instruments that have to be handled;
- Define the database path where data will be stored;
- Define the period (10 minutes currently used) for storing averaged data, this is the data acquisition cycle time;
- Obtain data (every 10 seconds currently set) for selected instruments within the data acquisition cycle:
  o For analog instruments (currently only the CM 11 Pyranometer), apply the calibration constants to translate the readings (voltages or currents) into analytical values;
  o Send commands to query instruments for data or keep listening the ports for instruments that have self defined output timing;
  o Scan instruments outputs to pick out the necessary data;
- Calculate average values and standard deviations for the cycle period;
- Query instruments for diagnostic data (when available), once every 10 minutes;
- Store all data in a database
  o With a single timestamp for the gas analyzers, FDMS-TEOM and Nephelometer
  o With the timestamp of their respective measurement for all other instruments.

The following instruments are managed with the DAS, using two PCs (currently called emepacq and emepacq2):

emepacq:

Devices for gas phase measurements:
- NO, NO_2, NO_x, 42C
- SO_2, 43C
- CO, 48C
- O_3, 49C

Devices for physical aerosol properties:
- Number size distribution for particles diameter >0.500 μm, APS
- On-line PM10 mass, FDMS-TEOM
- Aerosol light absorption, Aethalometer
- Aerosol light scattering, Nephelometer

emepacq2:

- Solar radiation
- Weather transmitter (temperature, pressure, relative humidity, wind speed and direction, precipitation)
- Precipitation data

- Particulate matter sampling data

A third PC (**emepacq3**) is dedicated to operate the LIDAR system, a fourth PC (**emepdma**) to operate the DMPS and to store its data directly to the database.

Data acquired with "emepacq" are currently stored on the central database **EmepDB** hosted on the PC **Lake**. Data acquired with "emepacq2" are locally stored on the same PC in a database called **EmepDB** as well. The PC "**Lake**" also connects the laboratory to the JRC network (Eidomain) via a radio bridge. The schematic setup of the data acquisition system is shown in Fig. 5.

The four containers at building 77p that make up the EMEP station are connected to each others by user configurable point-to-point lines (see Fig. 6).
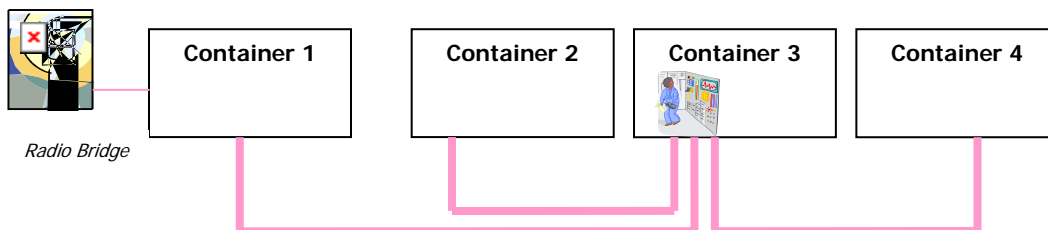
Fig. 6: interconnections of the laboratory container at the EMEP station

Trough these point-to-point connections, data are exchanged via TCP-IP, RS485 and RS232 protocols, depending on the instruments connected to the lines. To limit the number of necessary ports and improve the reliability of the long range serial communication, some RS 232 lines are converted to RS485 by means of CAS24 converters (from R.E. Smith, www.rs485.com).

The acquisition time is locally synchronized for all PCs via a network time server running on lake and is kept at UTC, without adjustment for summer/winter time. Data are collected in a Microsoft Access database, called EmepDB.mdb that runs on "**Lake**". This database is nightly backed-up by the IES back-up service.

Data evaluation

For evaluating the 2007 data, a structured data evaluation system (EMEP_Main.m) with a graphic user interface (see Fig. 7) has been developed using Matlab Release R2007b (www.mathworks.com) as the programming environment. The underlying strategy of the program is:

1) Load the necessary measurement data from all selected instruments from the data acquisition database as stored by the DAS (source database).
2) Apply the necessary individual correction factors, data analysis procedures, etc. specific to each instrument at the time base of the instrument.
3) Perform the calculation of hourly averages for all parameters.
4) Calculate results that require data from more than one instrument.
5) Store hourly averages of all results into a single Microsoft Access database, organized into different tables for gas phase, aerosol phase and meteorological data (save database).

In addition, quick looks of evaluated data for selected time periods can be produced as well as printed timelines in the pdf-format for the evaluated data. All database connections are implemented via ODBC calls to the corresponding MS Access database files.

With a second program (EMEP_DailyAverages.m), daily averages of all parameters stored in the hourly averages database can be calculated and are subsequently stored in a MS Access database as well.

Fig. 7: graphic user interface of the EMEP data evaluation program.

New container

During the second half of 2007, the following instruments for the physical characterization of aerosols moved into a new laboratory container at the EMEP station that is located north-west of the existing containers: Aethalometer, Nephelometer, Aerodynamic Particle Sizer, Differential Mobility Particle Sizer and LIDAR. The container is equipped with a new PM10 inlet and manifold that has been checked for particle losses. A characterization of this inlet will be presented in the EMEP report 2009.

Quality assurance

At JRC level the quality system is based on the Total Quality Management philosophy, the implementation of which started at the Environment Institute in December 1999. Lacking personnel to specifically follow this business, the JRC-Ispra air monitoring station did not renew the accreditation for the monitoring of SO_2, NO, NO_2 and O_3 under EN 45001 obtained in 1999. However, most measurements and standardized operating procedures are based on recommendations of the EMEP manual (1996), WMO/GAW, ISO and CEN standards. Moreover, the JRC-Ispra gas monitors and standards are checked by the European Reference Laboratory for Air Pollution (ERLAP) regularly (see specific measurement description for details). In contrast, no framework for audit and intercalibration of on-line aerosol instrument was in place in 2007. Within the EUSAAR project (http://www.eusaar.org), the Aethalometer and Nephelometer participated in an intercomparison exercise in Leipzig, Germany in March 2007.

Most of the other instruments were regularly calibrated through maintenance contracts.

The analytical laboratory of the JRC-Ispra station takes regularly part in the EMEP intercomparison exercise for rainwater analyses (see Fig. 8). Due to the use of new IC calibration standards in 2006, the bias for the different analytes in that year's EMEP laboratory intercomparison has been reduced drastically compared to the previous years.

Data quality for other measurements is also checked whenever possible through comparison among different instruments (for gases), mass closure (for PM), optical closure (DMPS/aethalometer/nephelometer), and ion balance (for precipitation) exercises.
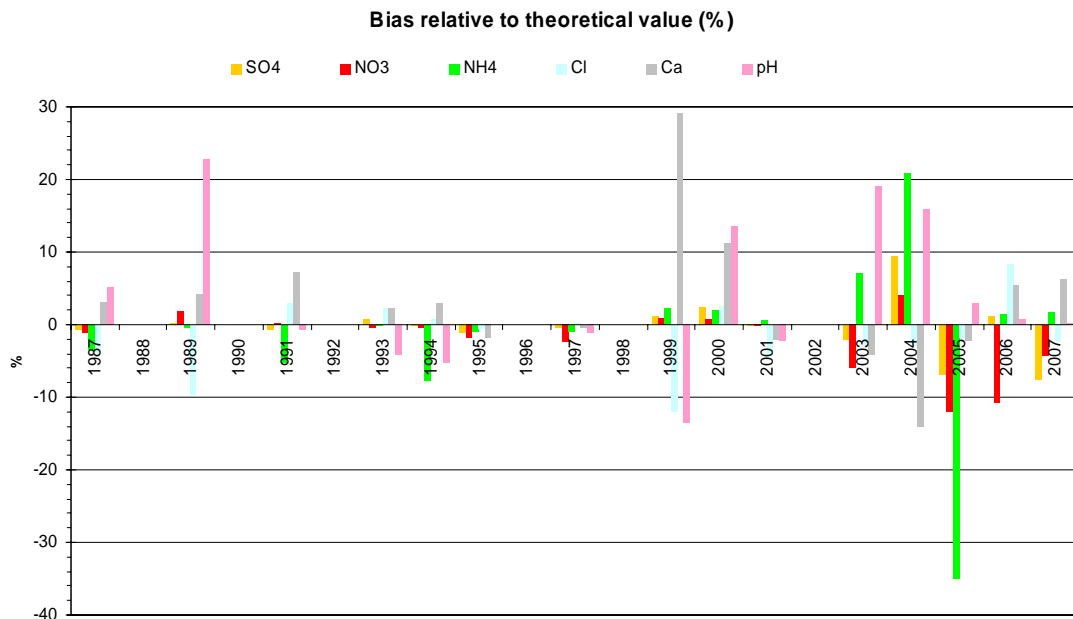
Fig. 8: JRC-Ispra results of the EMEP intercomparison for rainwater analyses.
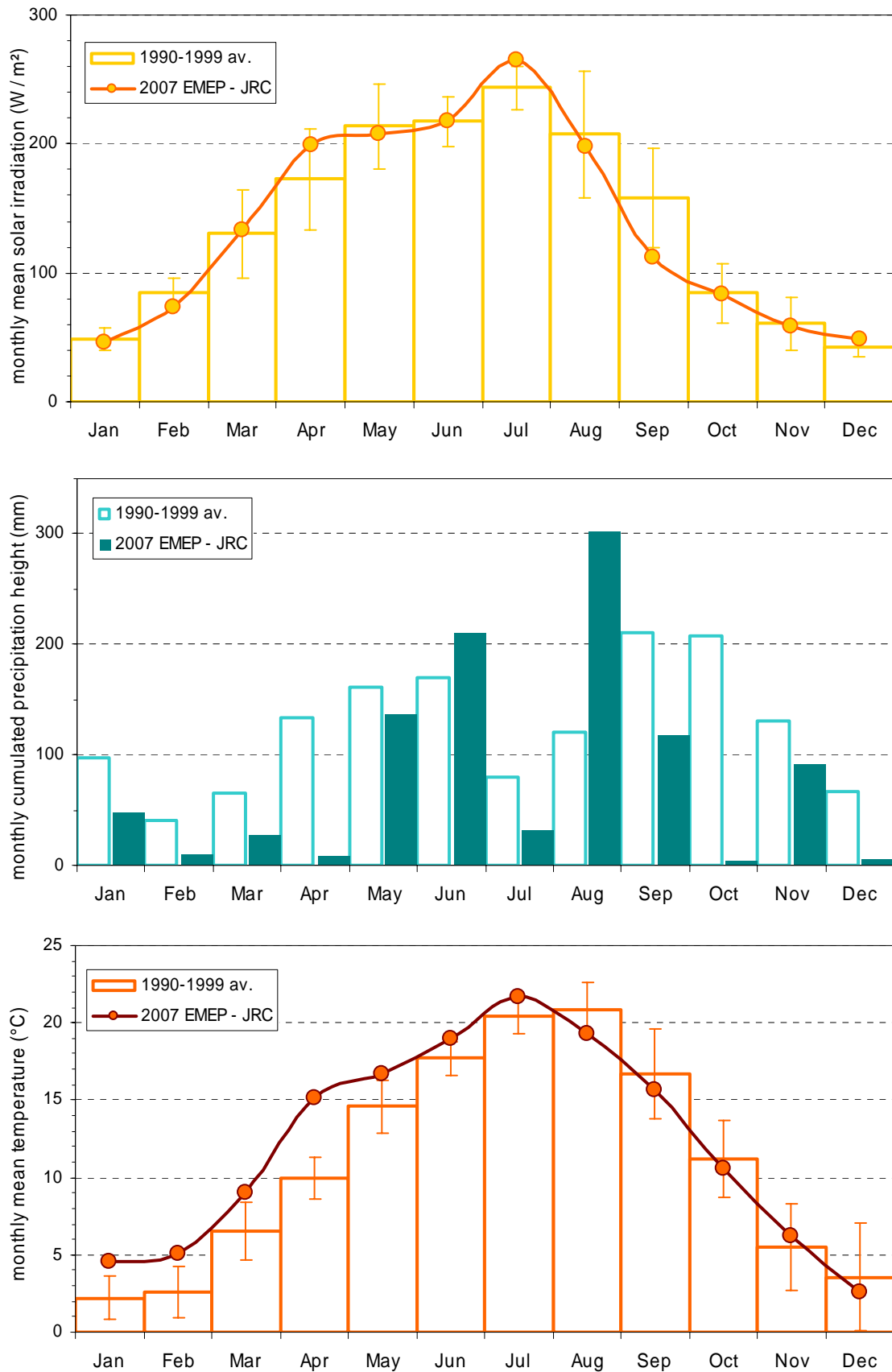
Fig. 9: solar global irradiation, precipitation amount, and temperature monthly means observed at the EMEP station in the JRC-Ispra, compared to the 1990-1999 period ± standard deviation

Results of the year 2007

Meteorology

Meteorological data were acquired directly at the EMEP site using the Vaisala WXT510 weather transmitter. Fig. 9 shows monthly values of meteorological parameters for 2007 compared to the 1990-1999 average used as reference period.

The monthly averaged solar radiation for 2007 follows the 1990-1999 average very well, except for July that was significantly sunnier and September that was much cloudier than during the reference period.

The total rainfall accumulated to 995 mm, so 2007 was a rather dry year again: 33 % less compared to the 1990-1999 average (1484 mm) and 98 mm (9 %) less than during 2006 (1093 mm). Especially April and October were very dry, for April also above average solar radiation and temperature have been recorded.

In 2007, only the summer months August and September were slightly cooler than during the reference period, the entire first half of 2007 however was significantly warmer. The temperature average over the whole year was 12 °C compare to 11 °C during 1990-1999.

Gas phase

Gas phase measurements were carried out over the whole year 2007. Unfortunately, the CO measurements encountered serious problems during the entire year, the instrument drifted. Due to a lack of sufficient calibration and zero point measurements, this drift could not be corrected for and thus CO data were not reliable. Therefore CO concentrations are not reported for 2007.

Seasonal variations in SO_2, NO, NO_2, NO_x and O_3 were comparable to those observed over the 1990-1999 period (Fig. 10), with higher concentrations during wintertime for primary pollutants, and higher concentrations in summer for O_3, resulting from photochemical atmospheric reactions.

SO_2 concentrations were generally approximately one third to one fourth as compared to the reference period and rather similar to 2006. NO_2 concentrations were slightly lower than observed during 1990-1999 and comparable to the 2006 level.
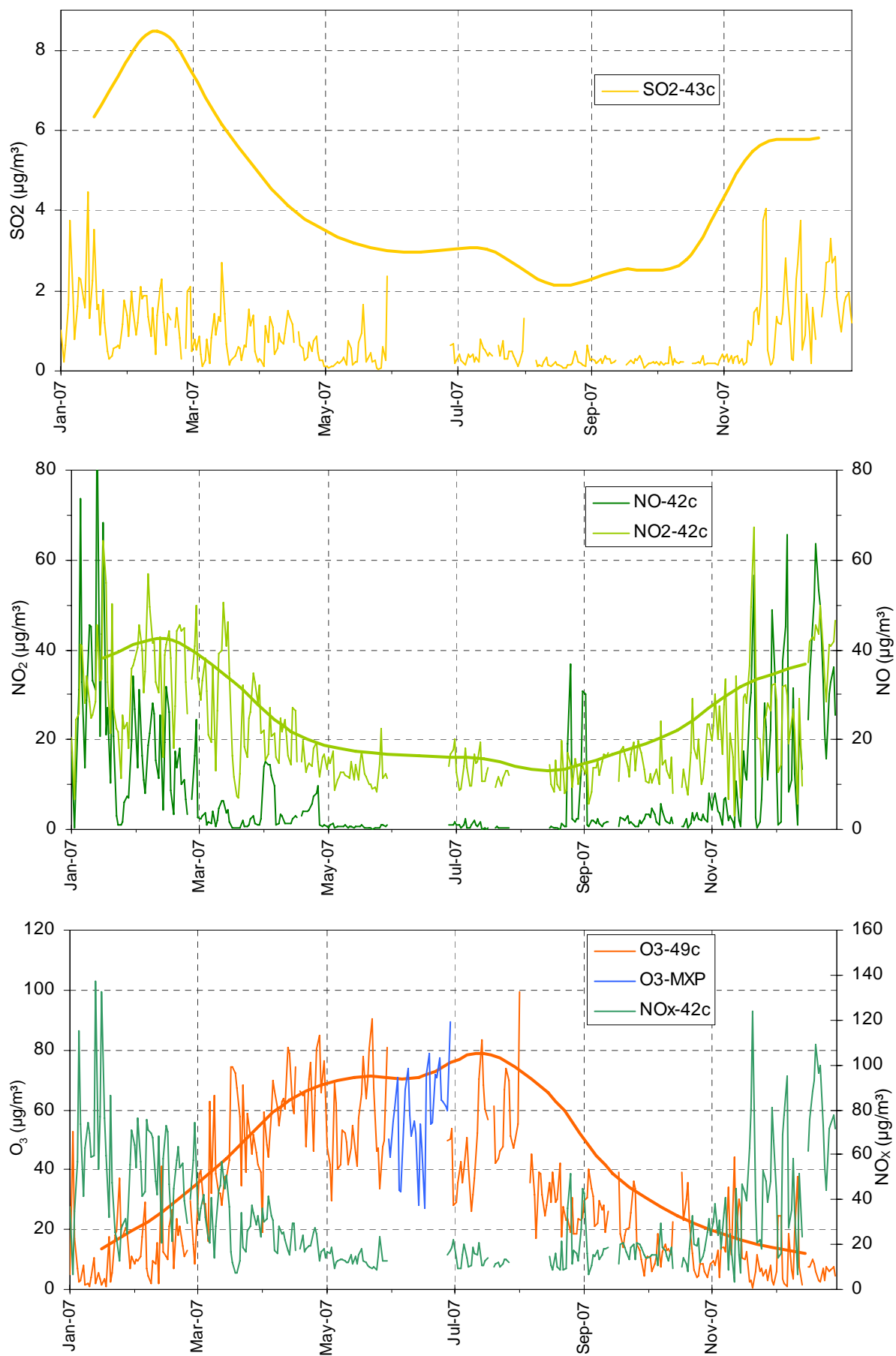
Fig. 10: variations of the 24 hr averaged concentrations of SO₂, NO₂, NO, O₃ and NOₓ in 2007 (thin lines) and 1990-1999 monthly averages (thick lines). June data for O₃ taken from Malpensa.

Concentrations of O_3 in 2007 were slightly lower compared to the reference period 1990-1999. To obtain a high data coverage that is important for all ozone exposure metrics, June concentrations measured by ARPA at Malpensa have been used. The high O_3 levels observed for a few days in January and February 2007 were all associated with high wind speed and low relative humidity, which characterize Foehn events and might lead to the transport of high altitude O_3 to the ground.

The low vegetation exposure to above the ozone threshold of 40 ppb (AOT 40) amounted to 9850 ppb h (with a data coverage for O_3 of 94 %), to be compared to 22230 ppb h for 2006 and 34000 ppb h / yr over the 1990-1999 decade (Fig. 11). The rather high AOT40 value for April and the low values for the summer months (92 % coverage) correlate very well with the high solar radiation (and temperature) for April and the rather high precipitation during the summer months of May till August.

SOMO35 (population exposure to above 35 ppb O_3) with 1590 ppb day was rather low in 2007 (Fig. 11) as compared to 2993 ppb day in the previous year. During 2007 (like in 2005), the O_3 population information warning level of 180 µg/m³ has never been reached. In the reference period 1990-1999 this warning level was exceeded 29 times per year on average.
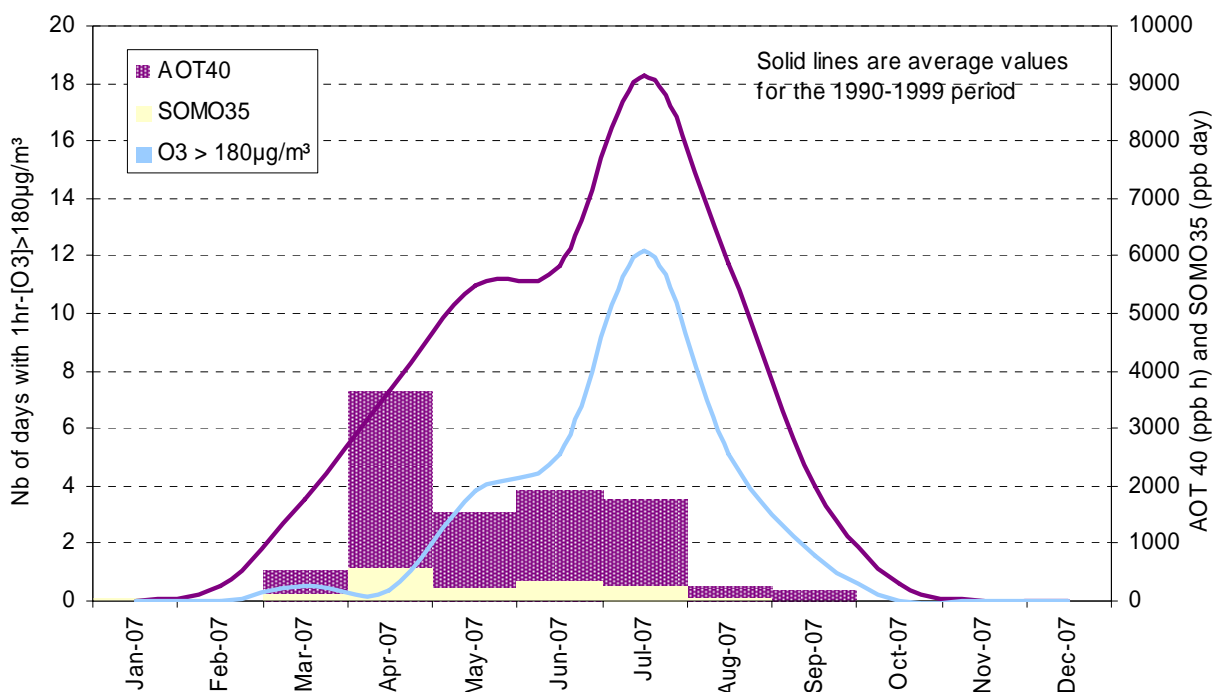
Fig. 11: AOT 40, SOMO35 and number of exceedances of the 1-hr averaged 180 µg/m³ threshold values in 2007 (bars), and reference period values 1990-1999 (lines)
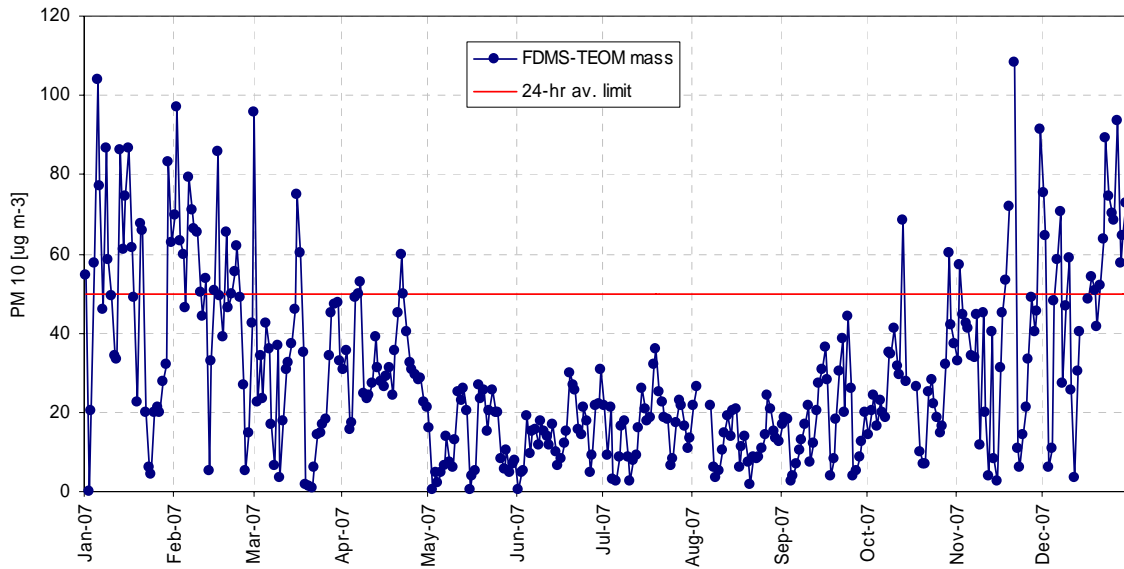
Fig. 12: FDMS-TEOM PM10 mass concentrations in 2007. The red line shows the 50 µg/m³24-hr limit value
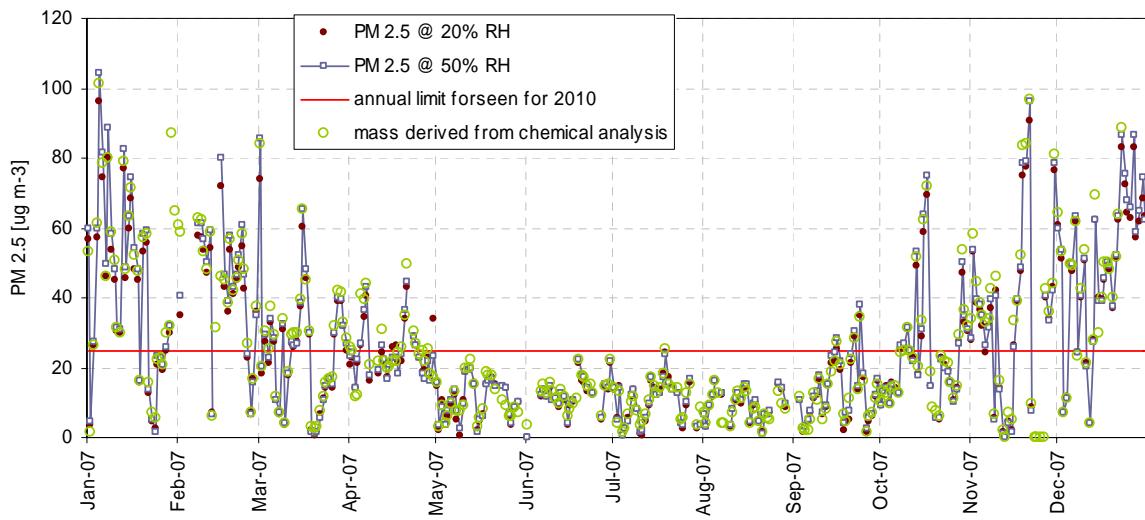
Fig. 13: 24hr-PM2.5 mass concentrations from off-line gravimetric measurements at 50 and 20% RH in 2007
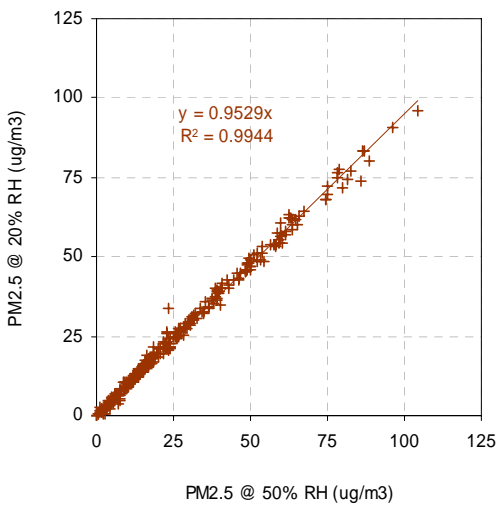
Fig. 14: regressions between gravimetric measure-ments at 20 and 50 % RH for PM2.5
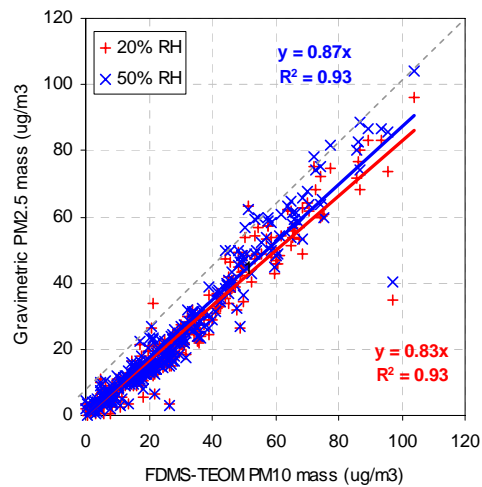
Fig. 15: regressions between FDMS-TEOM PM10 and gra-vimetric PM2.5 measurements at 20 and 50 % RH

Particulate phase

Particulate matter mass concentrations

PM10 annual mean concentration for 2007, measured with the FDMS-TEOM, was 29.5 µg/m³, 3.3 µg/m³ lower than 2006 and well below the European annual limit value of 40 µg/m³ (Fig. 12). The PM10 24-hr EU limit value of 50 µg/m³ has been exceeded 60 times (64 times in 2006), whereas the European directive **1999/30/EC** states that it should not to be exceeded more than 35 times a calendar year from 1st of January 2005 onwards. PM2.5 annual mean concentrations (Fig. 13) were 24.6 µg/m³ and 25.6 µg/m³, measured gravimetrically at 20 % and 50 % RH, respectively. These values were 2-3 µg/m³ lower than in 2006, the PM2.5 value was just around the envisaged European annual limit value of 25 µg/m³ that has to be reached by 2010.

The regressions between gravimetric measurements carried out at 20 and 50 % RH show that PM2.5 weighings at 20 % RH consistently lead to lower values than weighing at 50% (Fig. 14), suggesting that approximately 5 % of PM2.5 measured at 50 % RH consist of water.

On-line PM10 mass measurements were performed with the FDMS-TEOM for the whole year. The artefact correction taken into account by the FDMS ranged from -19.0 to +1.5 (av. = -4.0) µg/m³ over 24 hr with 30 positive values, compared to only a single one in 2006. On an hourly basis, sampling artefacts ranged from -23.9 to +11.8 µg/m³ with an average of -4.1 µg/m³, spikes excluded.

Comparing the PM10 mass measured with the FDMS-TEOM to weighed PM2.5 mass at 50 % RH (Fig. 15), it can be seen that PM2.5 contributes with 87 % to the total PM10 mass. The correlation with $R^2 = 0.93$ is quite good.

PM2.5 chemistry

Main ions (Cl^-, NO_3^-, SO_4^{2-}, $C_2O_4^{2-}$, Na^+, NH_4^+, K^+, Mg^{2+}, and Ca^{2+}), OC and EC were determined from the quartz fibre filters (for the whole year) collected for PM mass concentration measurements. During the warm season (5th of April till 30th of August), NO_3^- and NH_4^+ were measured from the cellulose filters as well.
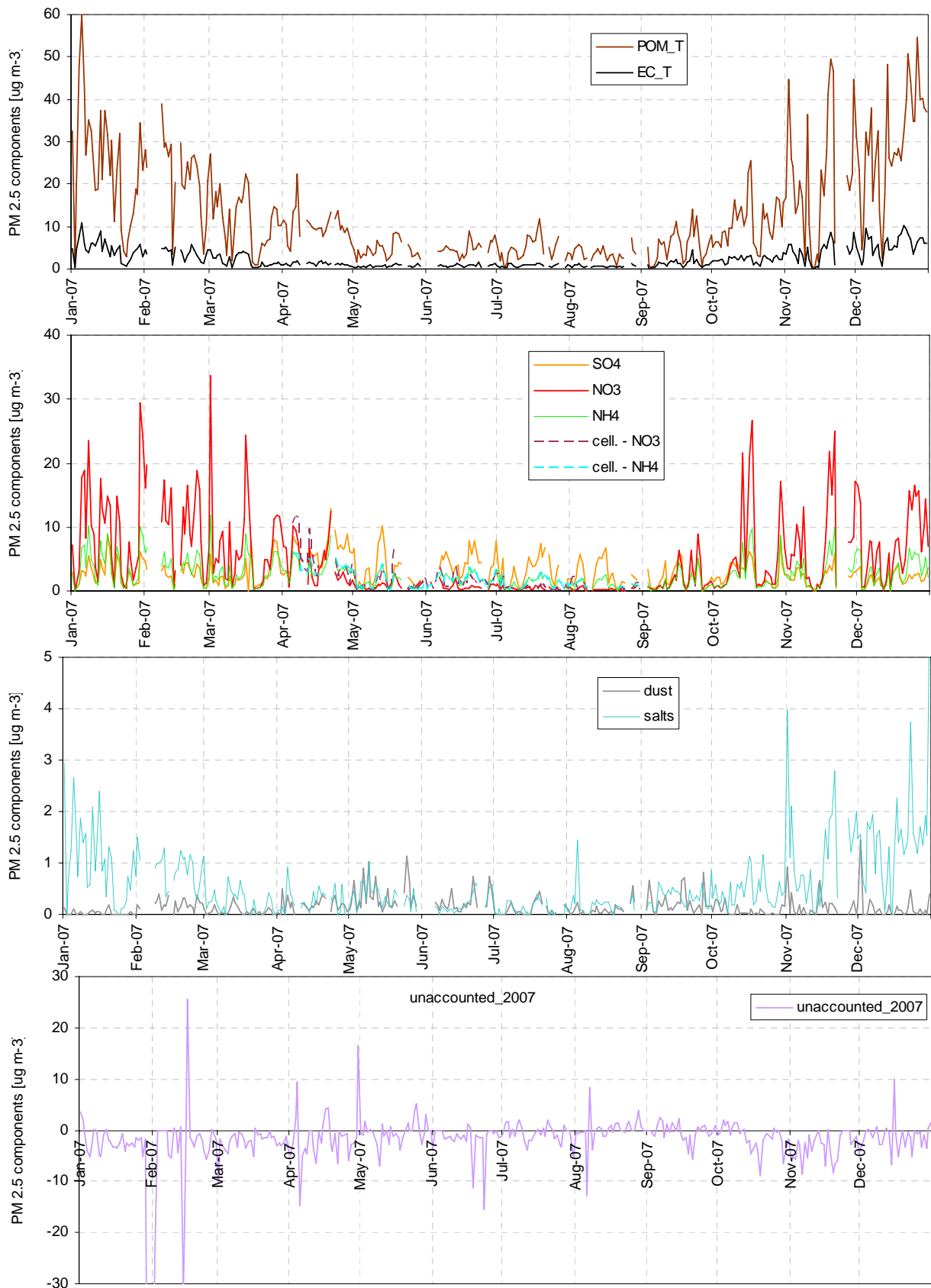
Fig. 16: 24-hr integrated concentrations of the main aerosol components in PM2.5 during 2007 (dashed lines on second plot indicate use of Whatman 40 cellulose filters for sampling)

Fig. 16 shows the temporal variations in the PM2.5 main components derived from these measurements. Particulate organic matter (POM) is calculated by multiplying OC values by the 1.4 conversion factor to account for non-C atoms contained in POM. "Salts" include Na^+, K^+, Mg^{2+}, and Ca^{2+}. Dust is calculated from Ca^{2+} concentrations and the slope of the regression found between ash and Ca^{2+} in the analyses of ashless cellulose filters (Whatman 40) in previous years (4.5). Most components show seasonal variations with higher concentrations in winter and fall, and lower concentrations in summer, like PM2.5 mass concentrations. This is mainly due to changes in pollutant horizontal and vertical dispersion, related to seasonal variations in meteorology. The amplitude of the POM, NH_4^+ and NO_3^- seasonal cycles may be enhanced due to equilibrium shifts towards the gas phase, and/or to enhanced losses (negative artefact) from quartz fibre filters during warmer month. Comparing the NO_3^- and $NH4^+$ concentrations determined from quartz and cellulose filters, average losses from April to August for NO_3^- on quartz filters were found to be 42 % (Fig. 17) and for NH_4^+ 21 %.

NH_4^+ follows NO_3^- + SO_4^{2-} very well as indicated by the regression shown in Fig. 18. This correlation results from the atmospheric reaction between NH_3 and the secondary pollutants H_2SO_4 and HNO_3 produced from SO_2 and NO_x, respectively.

The slope of this regression is very close to 1, which means that NH_3 was sufficiently available in the atmosphere to neutralise both H_2SO_4 and HNO_3. This furthermore indicates that PM2.5 aerosol was generally not acidic in 2007.
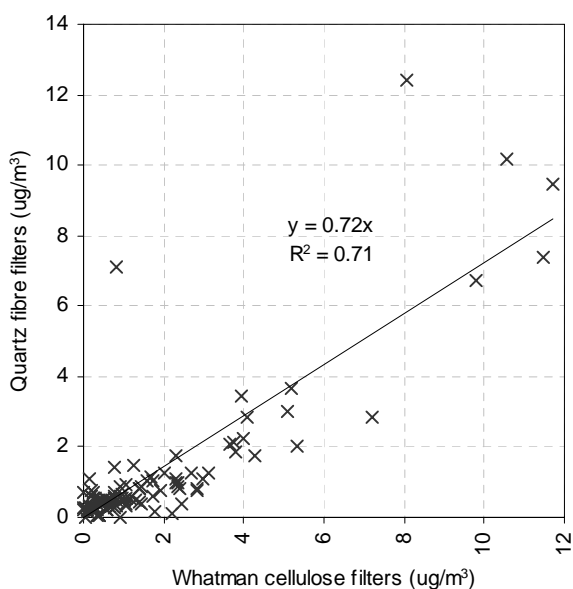
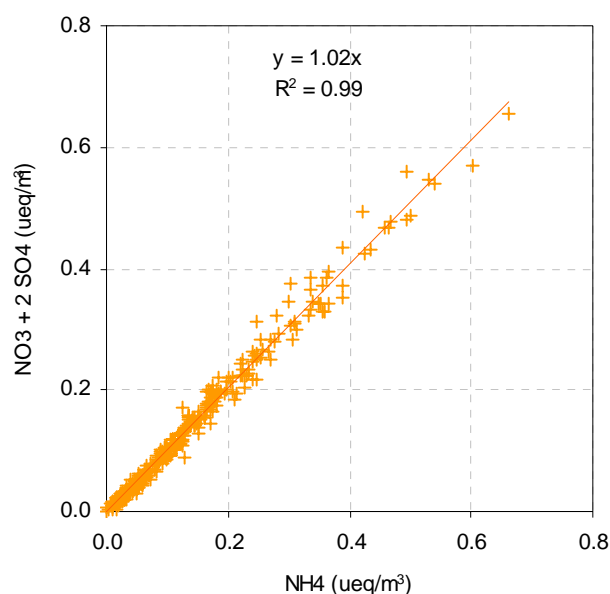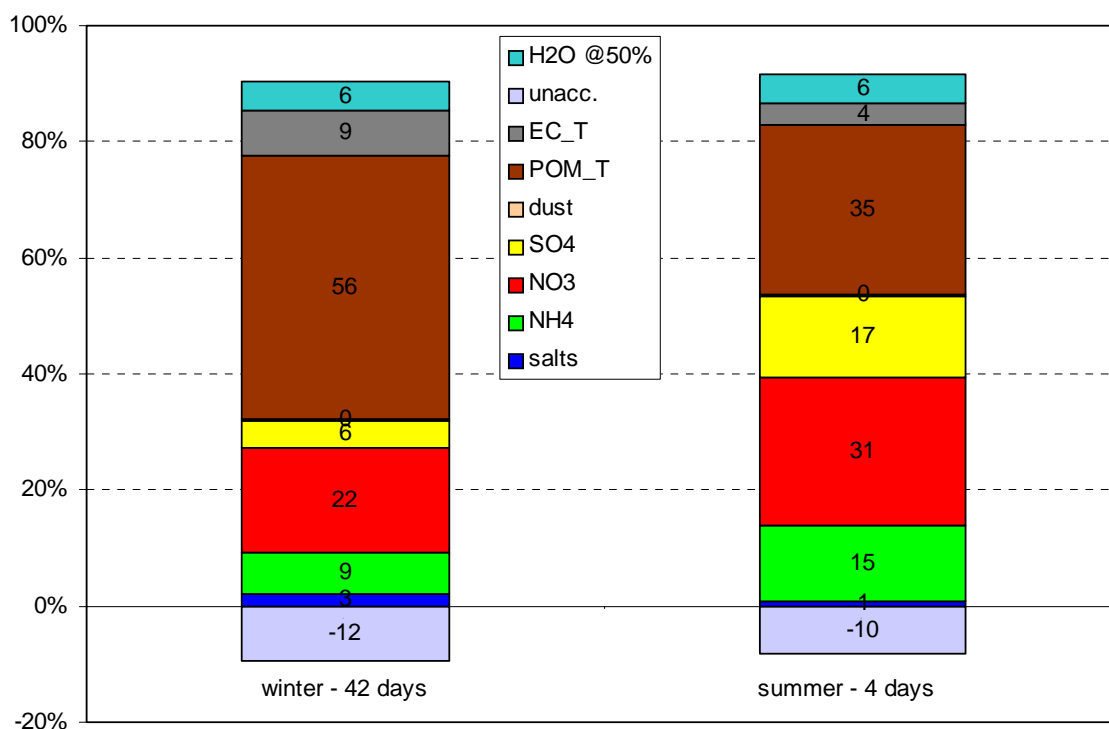*Fig. 17: NO₃- losses on quartz filters compared to cellulose filters during 2007*

Fig. 18: SO₄²⁻ + NO₃⁻ vs. NH₄⁺ (µeq/m³) in PM2.5 for 2007
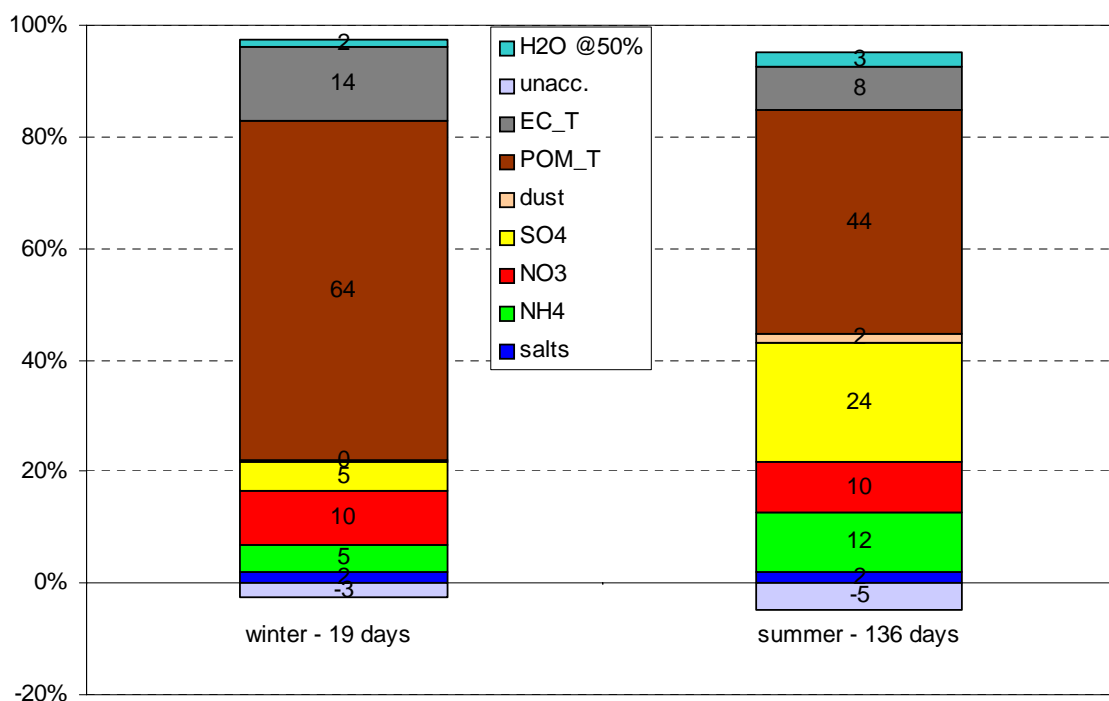
Fig. 19: average composition of PM2.5 for days during which PM10 > 50 µg/m³(top) and PM10 < 25 µg/m³(bottom), in winter (Jan., Feb., Dec.) and extended summer (Apr. – Oct.)

<u>Contribution of the main aerosol components to PM2.5 during high and low PM10 concentration periods observed in winter and (extended) summer</u>

The contributions of the main aerosol components to PM2.5 is presented (Fig. 19) for days on which the 24-hr limit value for PM10 of 50 µg/m³ was exceeded, in winter (Jan., Feb. and Dec., 42 cases) and extended summer (Apr. to Oct, 4 cases).

These PM2.5 compositions may not always represent accurately the actual composition of particulate matter in the atmosphere (due to various sampling artefacts), but are suitable to assess which components contributed to the PM2.5 mass concentration when measured according to the normative rules described in EN12341 (i.e. 50 % RH).

During wintertime, carbonaceous species (POM and EC) represented a much larger fraction of PM2.5 (65 % for high PM10, 78 % for low PM10) than secondary inorganic species NH_4NO_3 and $(NH_4)_2SO_4$ (37 % for high PM10, 20 % for low PM10). Water accounted for 6 % and 2 % of the PM2.5 mass during high and low PM10 episodes, respectively.

During the extended summer season (Apr. to Oct.), carbonaceous species (POM + BC) contributed with 39 % and 52 % to the PM2.5 mass during high and low PM10 periods, which is less compared to the composition in winter. Inorganic secondary species (NH_4NO_3 and $(NH_4)_2SO_4$) made up for 63 % and 46 % of PM2.5. Water accounted for 6 % and 3 % of the PM2.5 mass measured at 50 % RH, a similar amount as in winter.

Dust and salts do not contribute significantly to the PM2.5 mass as these particles are not predominant in the Po valley region and are also more likely found in the coarse particle fraction.

Summarizing the composition of PM2.5 for polluted days in summer and winter, the contribution of carbonaceous components (POM and EC) was significantly lower as compared to cleaner days. In contrast, more secondary inorganic components were found. This suggests a relatively smaller contribution of local sources to PM2.5 during polluted days, whereas secondary (regional) aerosol contribution is larger. The differences in particle compositions in Ispra for polluted and very clean days, i.e. during Foehn events, have been extensively described in Mira-Salama 2008 and used to characterize urban and regional sources of particles.

<u>PM10 chemistry</u>

PM10 has been collected and analyzed for a total of 31 filters in 2007. Fig. 20 indicates a rather good correlation of the daily averaged on-line mass measurement with the FDMS-TEOM and the filter based methods with both filter weighing and chemistry derived masses. For small masses though the methods give significantly different results, the FDMS-TEOM masses are lower. Comparing weighed PM2.5 and PM10 masses shows that PM2.5 makes up for 82 % of the total PM10 mass (Fig. 21).

Furthermore looking at the chemical analysis of the PM10 and PM2.5 filters, the correlations of Fig. 22 indicate that the contributions of NH_4, SO_4 and POM to PM10 and PM2.5 are the same. NO_3 is more present in PM10 (approx. 70 % of NO_3 is found in PM2.5 compared to a 82 % of the total mass) and all EC, on the other hand, is found in PM2.5. The correlation coefficients though are not high for all compounds; the number of samples with only 31 limited.
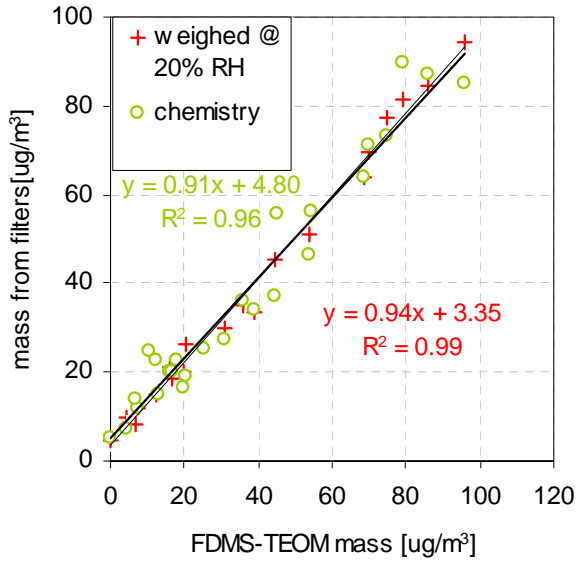

Fig. 20: regression between PM10 mass from FDMS-TEOM and weighed (crosses) and chemistry derived (circles) PM10 masses
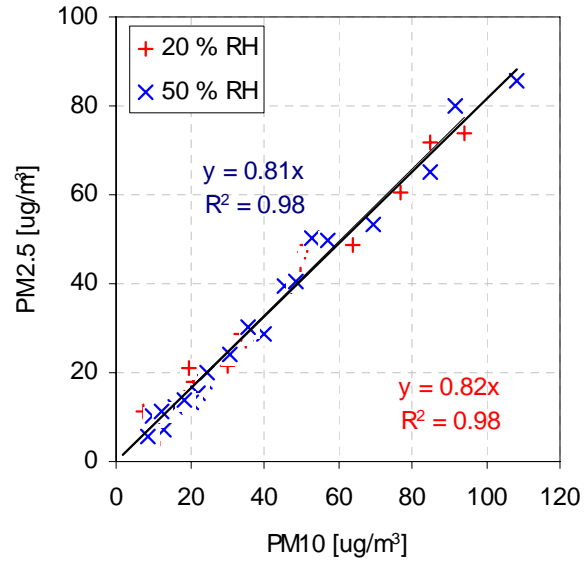
Fig. 21: regression between weighed PM10 and PM2.5 at 20 % (red) and 50 % RH (blue)
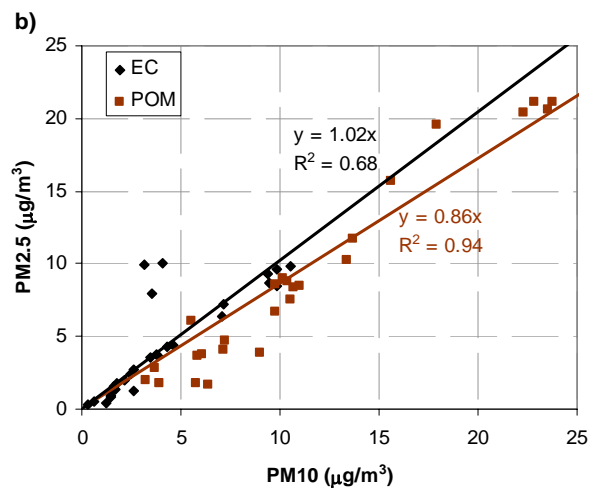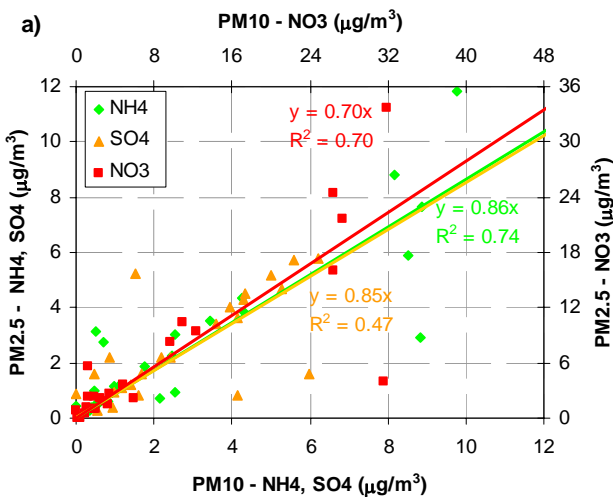
Fig. 22: correlation between chemical composition of PM10 and PM2.5, Panel a) NH_4, SO_4 and NO_3, b) elemental carbon (EC) and organic matter (POM)
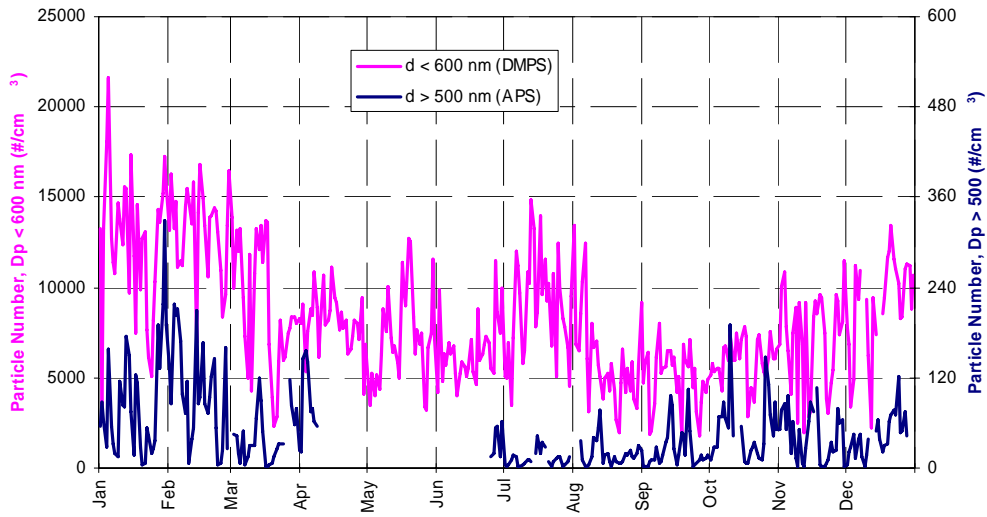
Page left intentionally blank

Fig. 23: 24 hr - averaged particle number concentrations for Dp > 500 nm and Dp< 600 nm
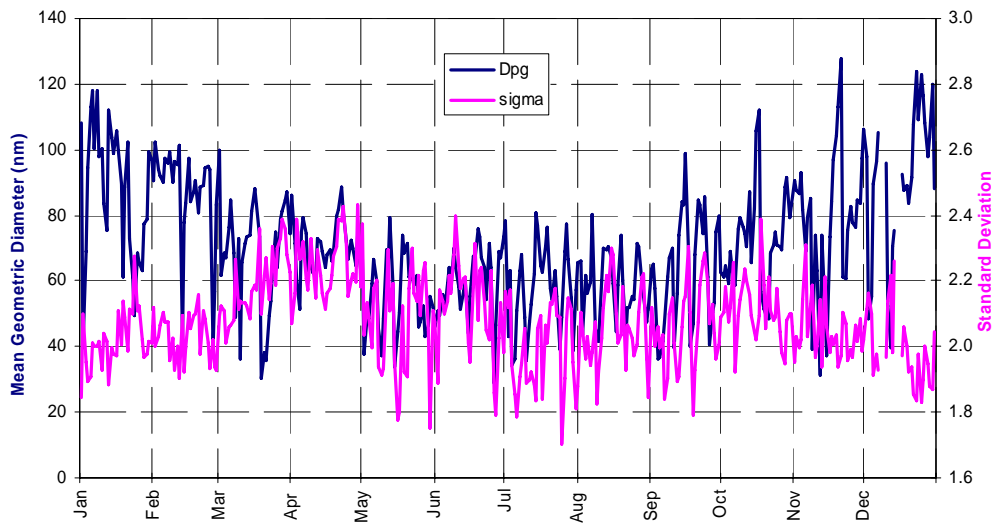

Fig. 24: 24 hr - averaged particle geometric mean diameter (measured with DMPS) and standard deviation
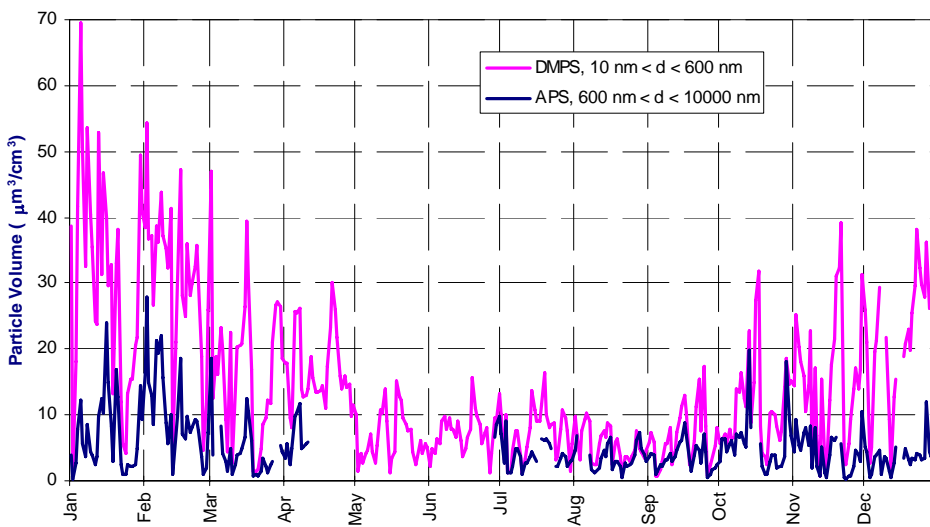

Fig. 25: 24 hr - averaged particle volume concentrations for Dp > 500 nm and Dp < 600 nm

<u>Aerosol physical properties</u>

Measurements of the particle number size distributions smaller than 600 nm diameter were carried out using a Differential Mobility Particle Sizer over the whole year 2007. Particle number concentrations averaged over 24 hr (from 08:00 to 08:00 UTC) ranged from 1800 to 22000 cm^{-3} (average: 9200 cm^{-3}) and followed a seasonal cycle comparable to that of PM mass concentration, with maxima in winter and minima in summer (Fig. 23).

The variations in particle number size distributions parameters at RH < 30 % (*Fig. 24*) show seasonal patterns as well: the mean geometric diameter is generally larger in winter than in summer, whereas the standard deviation of the distribution follows an opposite trend (larger in summer than in winter). The size distribution of particles larger than 500 nm was measured using an Aerodynamic Particle Sizer (aerodynamic converted to geometric diameter using a particle density of 1.50). As previously observed, particles larger that 500 nm accounted for a very small fraction of the total particle number only, on average for 0.6 % (*Fig. 23*), but for 27 % of the total particle volume (*Fig. 25*). The seasonal variations in particle volume concentration reflect the changes in particle number and mean geometric diameter, with larger volumes in winter than in summer. Looking at particle number size distributions reveals a good agreement among the APS and the DMPS across the 4 seasons of the year (*Fig. 26*).
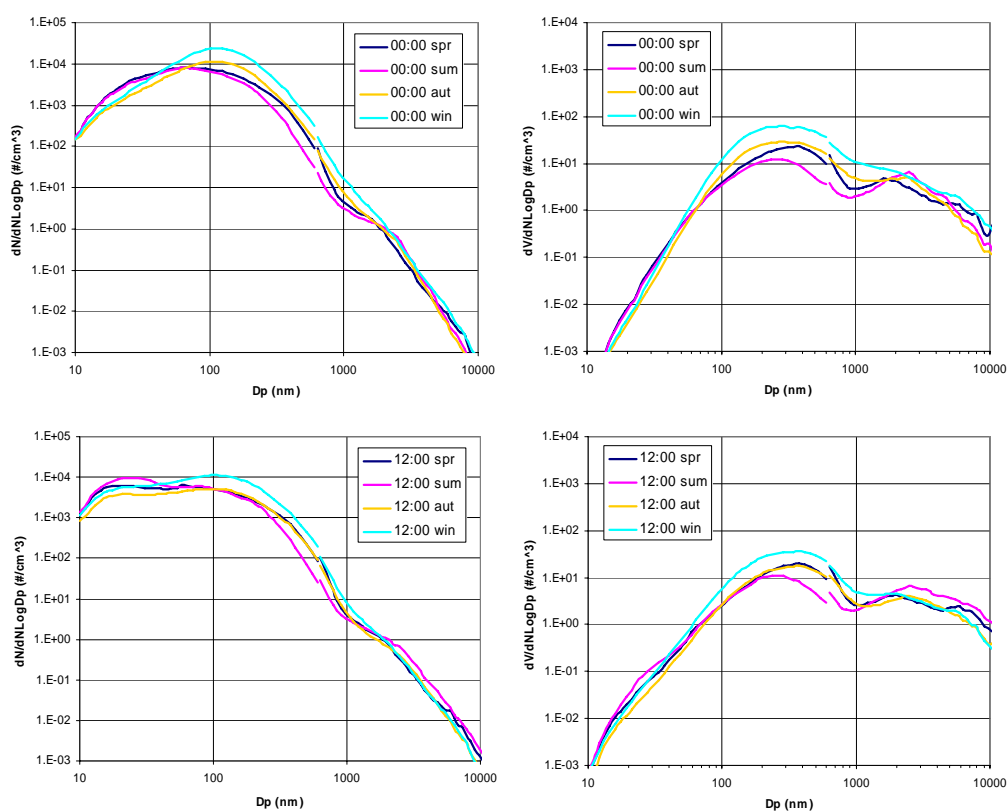

Fig. 26: seasonal mean particle number (left) and volume (right) size distributions at 00:00 (top) and 12:00 UTC (bottom) measured with a DMPS (10-600 nm) and an APS (0.6-10 µm, density of 1.5 g/cm3 assumed for conversion of aerodynamic diameter)
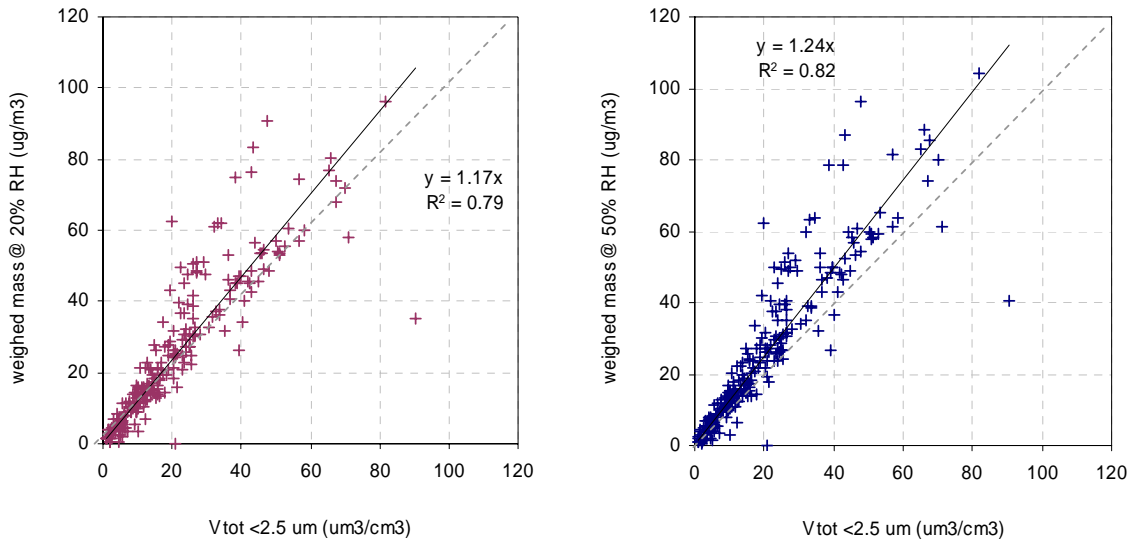
Fig. 27: regressions between PM2.5 mass concentrations determined from gravimetric measurements at 20 % RH (left) and 50 % RH (right) and particle volume (Dp < 2.5 µm) calculated from DMPS and APS measurements
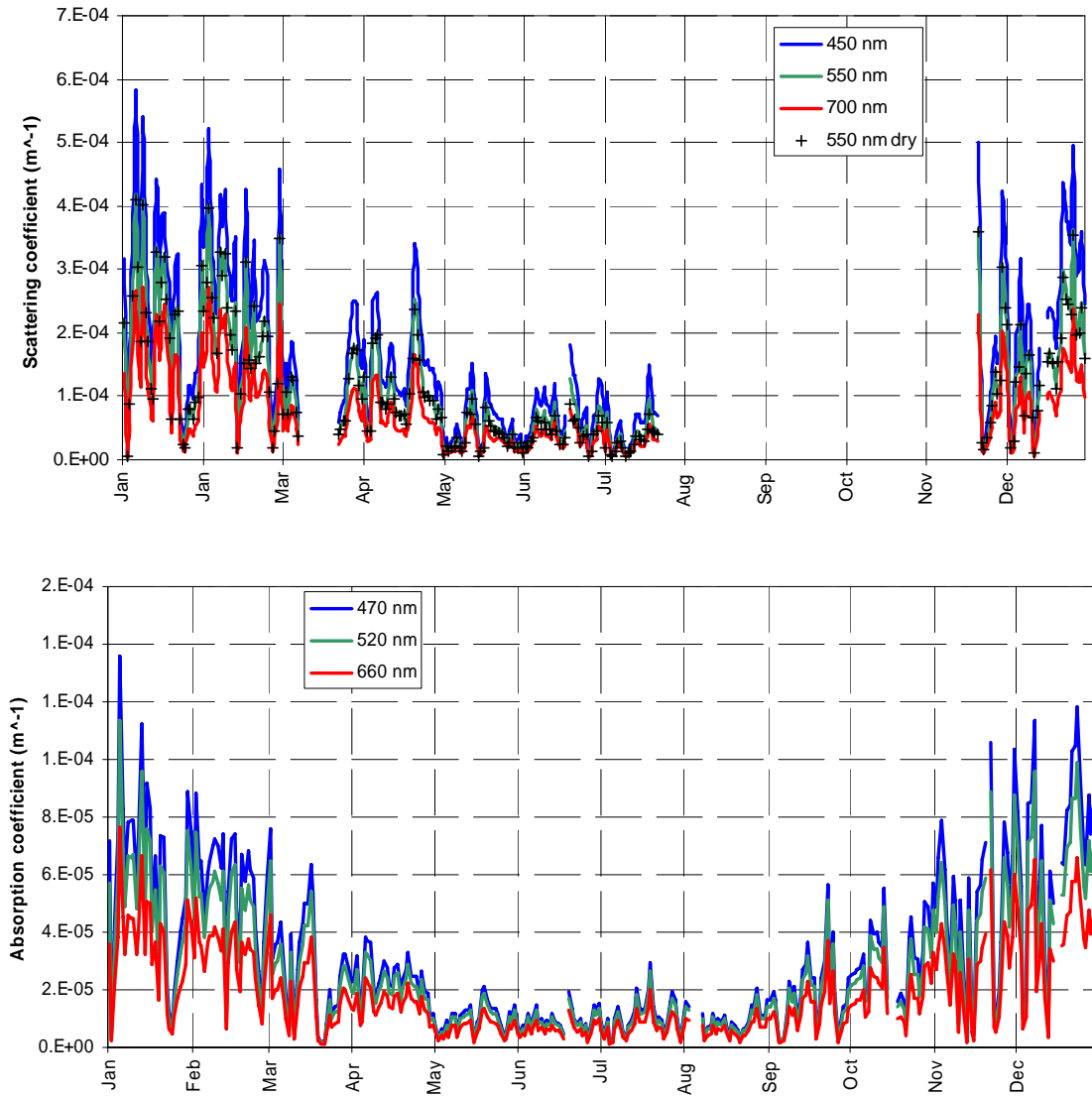

Fig. 28: daily mean atmospheric particle scattering (top) and absorption (bottom) coefficients at three wavelengths, derived from Nephelometer and Aethalometer measurements (not corrected for RH, except if specified)

The comparison between PM2.5 mass and aerosol volume concentration (for d < 2.5 μm) shows good correlations (Fig. 27). The slope of the regression between PM2.5 at 20 % RH and particle volume suggests an aerosol density close to 1.2, significantly lower than the 1.5 measured in 2005. Particles bigger than 600 nm make up for only 27 % of the total volume, compared to 36 % in 2005, and therefore the overestimation of the total volume is probably not caused by the APS instrument. On the other hand, an aerosol density of 1.2 is too low compared to the results from the previous years. Regressions between the aerosol extinction coefficient with mass and volume (see Fig. 30), indicate that their might be problems with the volume measurements. Summarizing, as in 2006 a satisfying explanation for this high particle volume cannot be given.

Aerosol optical properties

Aerosol optical properties have been monitored continuously during 2007 (Fig. 28). Due to software bug in the data acquisition system, Nephelometer data are not correct from 23rd of July till 20th of November. Data from the Nephelometer TSI 3563 have been corrected for angular non idealities (truncation to 7 – 170°, slightly not cosine-weighted distribution of illumination) according to Anderson and Ogren (1998). The equations linking the correction factor and the Ångstrom coefficient established for sub-μm particles (Anderson and Ogren, 1998) were used for correcting total scattering, since the median sub-μm mass fraction was 0.82 in Ispra for 2007. This leads to a quite conservative correction (+5-11 % for scattering, ca -5 % for backscattering). However, the Nephelometer was operated without RH control, but RH inside the Nephelometer was recorded during the year. It was observed that the RH in the Nephelometer exceeded 60 % only in the period from the 4th of June till 5th of October. At such a RH, scattering coefficients are 25 % larger than in dry conditions, based on calculations accounting for a mean refractive index derived from chemical composition, the Ångstroem coefficient, and the Mie theory (Nessler et al., 2005). For 2007, corrections for RH were <20 % for 94 % of all hourly averaged measurement values and for 92 % of the 24-hr averages.

Atmospheric particle absorption coefficients were derived from the Aethalometer AE-31 data corrected for the shadowing effect when Nephelometer data were available, and for the multiple scattering occurring on/into the Aethalometer filter according to Schmid et al. (2006). The correction factors we used were 3.6, 3.65 and 3.95 for blue, green and red light, respectively. Corrections for the shadowing effect were +10 % on average (< +17 % for 90th percentile).
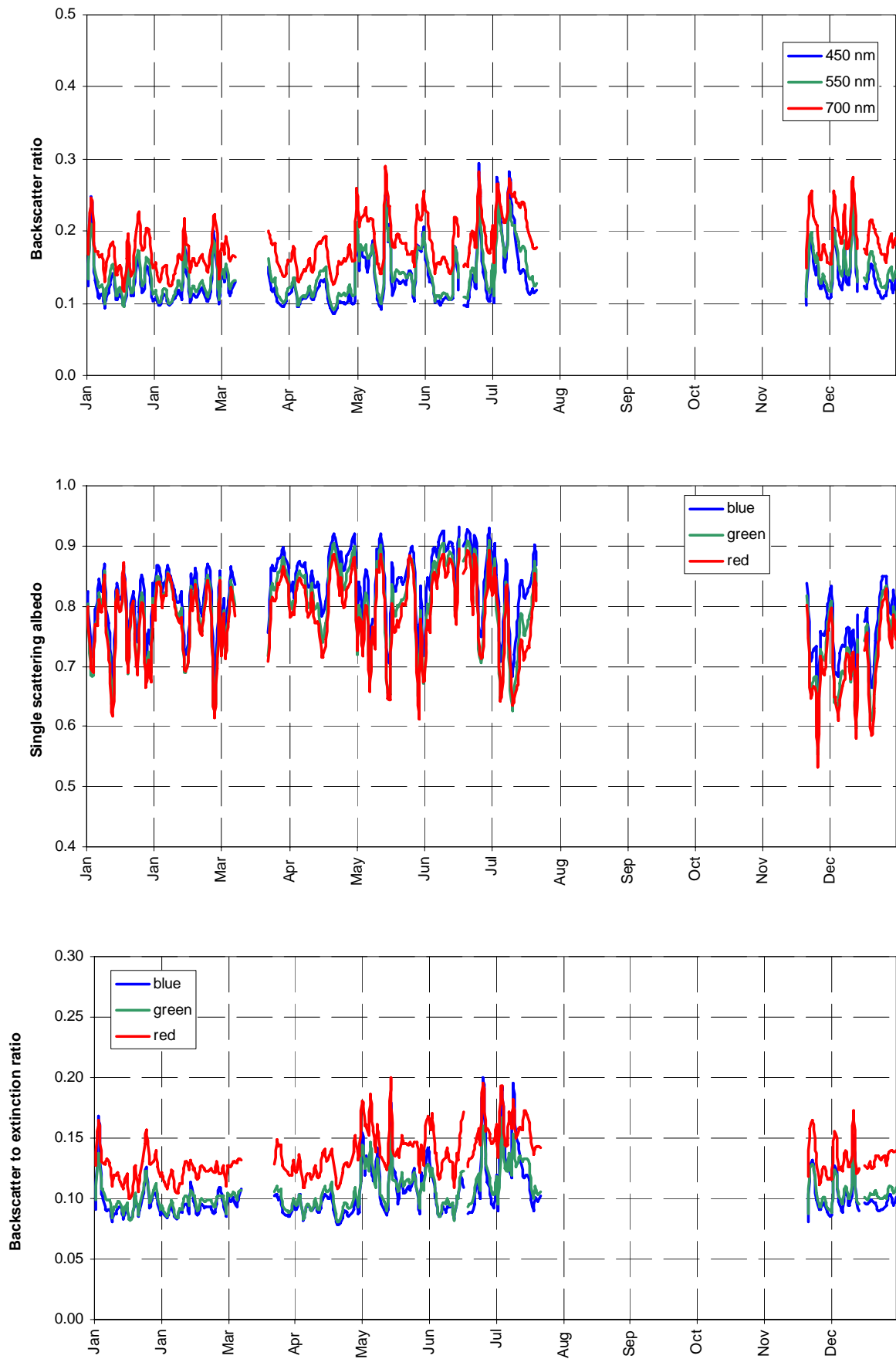
Fig. 29: aerosol 24-hr average backscatter to total scatter ratio, single scattering albedo and backscatter to extinction ratio at three wavelengths corresponding to blue, green and red (RH generally < 40%)

Therefore, possible biases in scattering coefficient determination are not expected to affect the determination of the aerosol absorption coefficient significantly. The uncertainty of the multiple scattering correction factor may introduce a much larger uncertainty in the aerosol absorption coefficient values, since correction factors ranging from 2 to 4 have been proposed (Weingartner et al., 2003; Arnott et al., 2005).

It should be noted that the use of the correction coefficients proposed by Schmid et al. (2006) leads to aerosol absorption coefficients equal to 83 % of the PSAP-matched aerosol absorption coefficients calculated from the regression found in the Aethalometer manual (version 2003.04, p.11): PSAP abs. coef. $[Mm^{-1}]$ = 10.78 EBC $[\mu g\ m^{-3}]$.

Both scattering and absorption coefficients follow seasonal variations (Fig. 28) in line with PM mass variations, mainly controlled by pollutant dispersion rates. The backscatter / total scatter ratio generally ranged from ca. 10 to ca. 30 %, (Fig. 29). The 24 hr averaged single scattering albedo for green light (at RH generally <40 %) ranged from 0.55 to 0.91 (annual average 0.79). The aerosol extinction coefficient was calculated as the sum of the scattering and absorption coefficients. Compared to the 2007 measurements, no change in optical particle properties has been observed during 2007.

The aerosol extinction coefficient and particle mass or volume concentrations are rather well correlated (Fig. 30). The slope of the regression between extinction and mass shows that the extinction mass efficiency is on average 4.5 $m^2 g^{-1}$, to be compared with 4.7 $m^2\ g^{-1}$, the value calculated based on the aerosol mean chemical composition during 2007, and mass cross section coefficients for the various constituents found in the literature (Table 2).
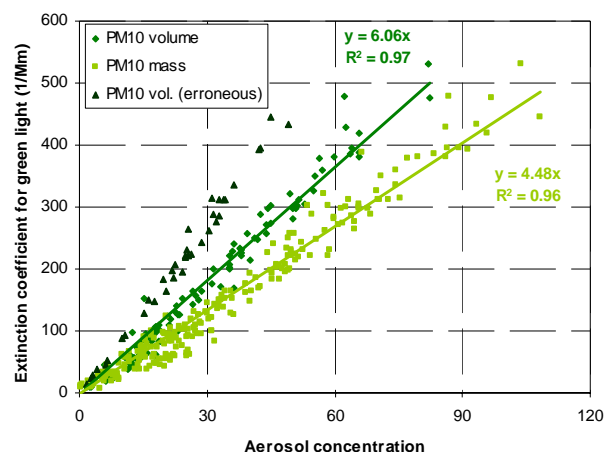

Fig. 30: regressions between the aerosol extinction coefficient and PM10 mass (FDMS-TEOM) and volume (DMPS + APS) concentrations. Erroneous volume data from 9.11.-31.12

Table 2: mean aerosol chemical composition (PM2.5) in 2007 and extinction efficiency.

The slightly low slope of 6.1 of the extinction to volume correlation stems most likely from too high volume measurements as described in the previous section 'Aerosol physical properties'. The erroneous volume data from 9.11.-31.12. are shown for completeness.

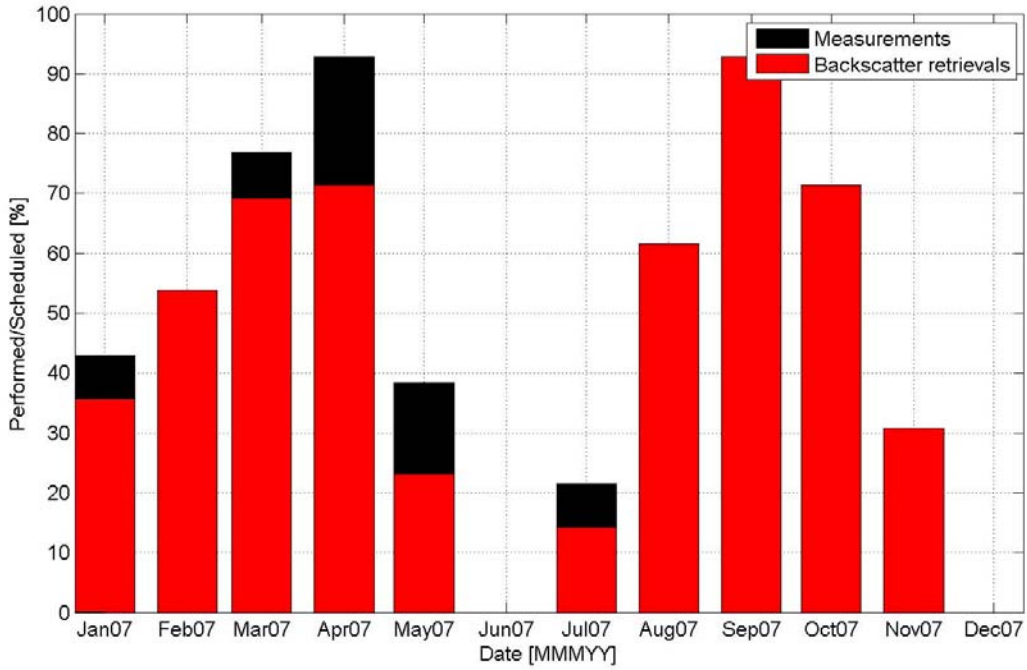|	2006 PM2.5 comp.	σ_{ext}	Reference
	(%)	(m²/g)	(for σ_{ext})
"sea salt"	2	1.3	Hess et al., 1998
NH_4^+, NO_3^- and SO_4^{2-}	39	5.0	Kiehl et al., 2000
organic matter	49	3.6	Cooke et al., 1999
black carbon	9	11	Cooke et al., 1999
dust	1	0.6	Hess et al., 1998
total	100	4.7	

43

Fig. 31: Percentage of LIDAR measurements performed for EARLINET (black) and evaluated and sub-mitted (red) for 2007
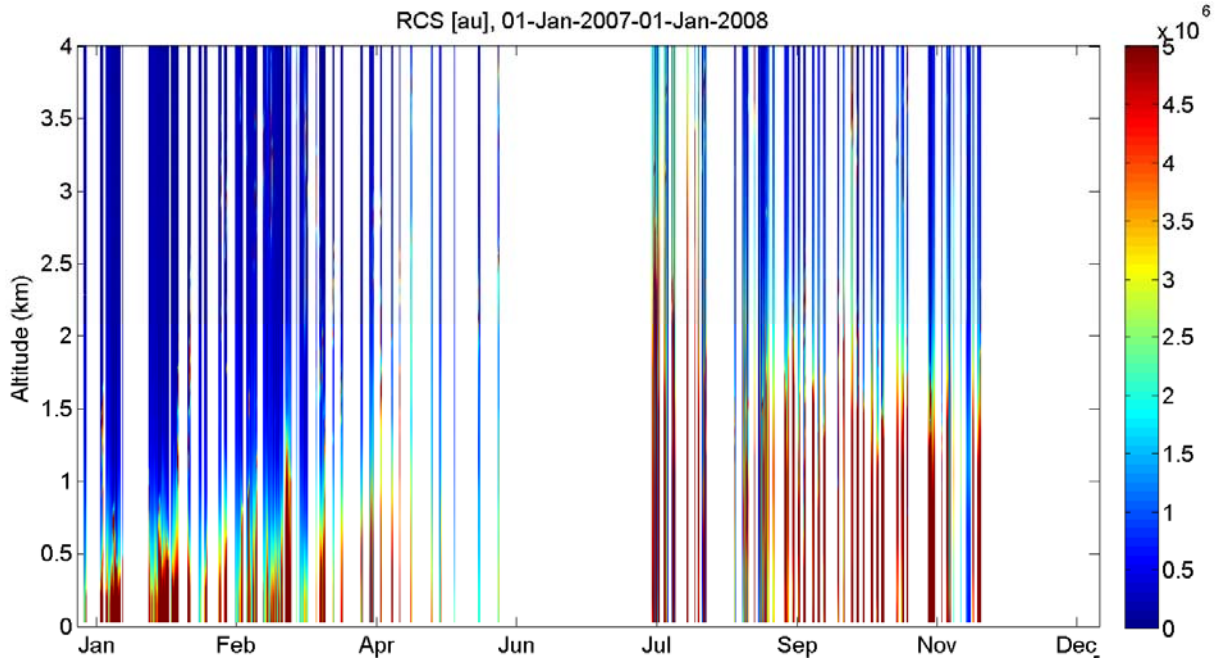

Fig. 32: six hour averages of LIDAR RCS profiles for 2007. The white areas signify the absence of the measurements.

LIDAR measurements – *v*ertical profiles of aerosol optical properties

Aerosol backscatter and extinction profiles have been derived from CIMEL LIDAR measurements in 2007 whenever the weather situation was favourable, i.e. no rainfall and no low clouds present, and except for two longer periods in June / July and November / December due to instrumental problems.

With the CIMEL LIDAR the JRC EMEP station participates as associate member in the EARLINET-ASOS project (www.earlinet.org). In order to establish a climatology of LIDAR derived aerosol optical profiles, measurements were scheduled Mondays at 14:00 local solar time (+/- 1 h), at sunset (-2 h, +3 h) and Thursdays at sunset (-2h, +3h). Additionally to these regular measurements, measurements taken during the overpass of the CALIPSO satellite (http://www.nasa.gov/mission_pages/calipso/main/) are reported to EARLINET as well. Fig. 31 shows the percentage of regular LIDAR measurements that were performed and evaluated / submitted to EARLINET. Missing measurements were due to low level clouds (28 %), rain (25 %), instrumental problems (32 %) and others (15 %).

Fig. 32 shows the 6 hour averages at a vertical resolution of 60m of the RCS profiles for the entire year. The plot shows the usual trend of the PBL height for the Po Valley region, which is smaller during winter and higher during summer. While during winter, the PBL height is around 500m – 1000m, during summer, it increases to approximately 1500m. However, large values can be observed during autumn as well.
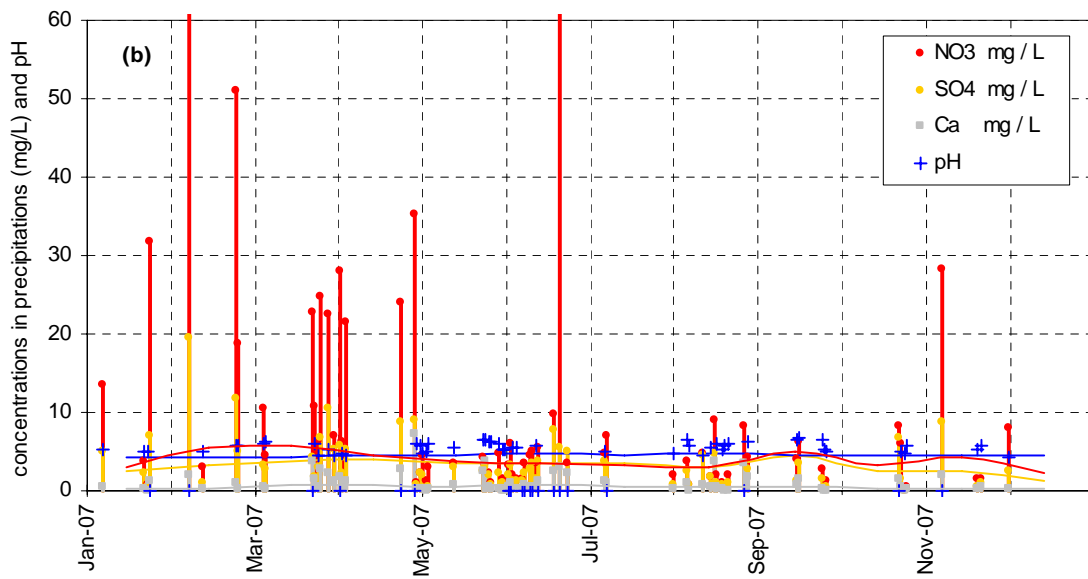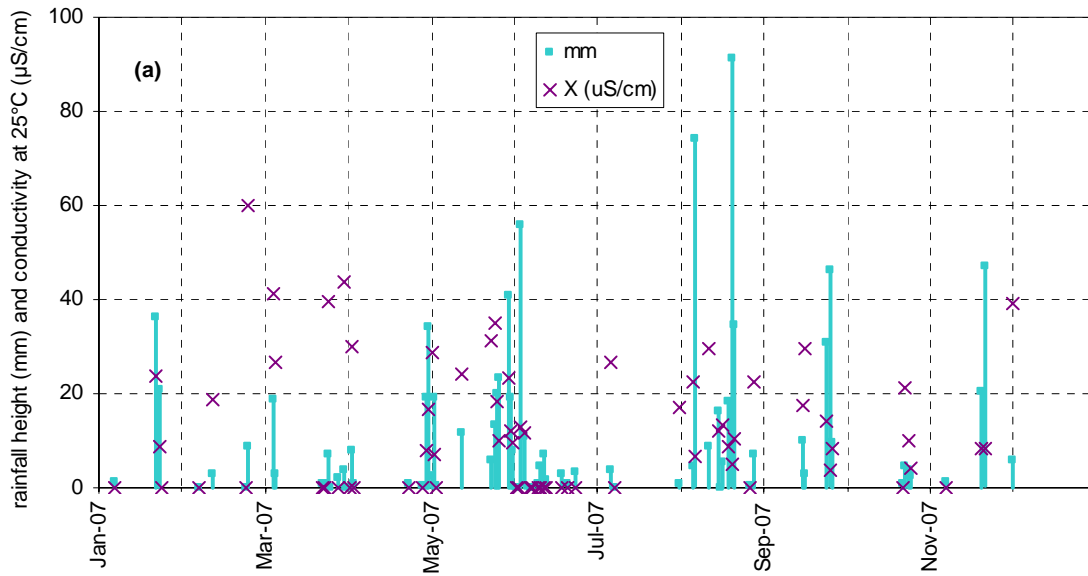
Fig. 33 : (a) precipitation amount, conductivity and (b) concentrations of 3 main precipitation components and pH recorded in 2007 (bars and crosses) and during the 1990-1999 period (lines)
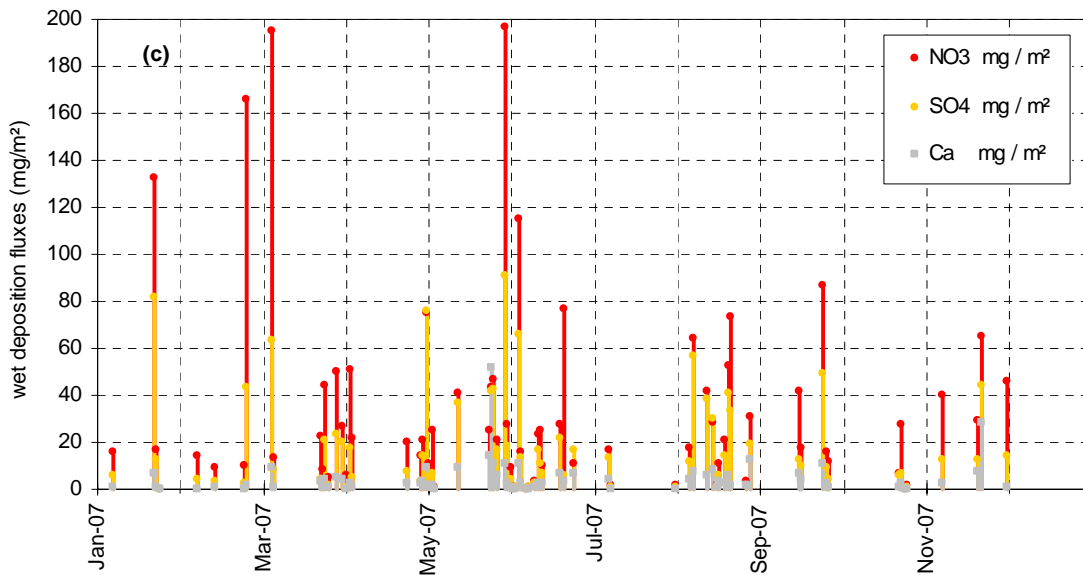

Fig. 34: wet deposition fluxes of 3 main components in rain water in 2007

Precipitation phase

In 2007, 74 precipitation samples were collected and their ion content determined. The pH-values for 52 and the total conductivity for 45 of those samples were measured, not sufficient water volume was available for the remaining samples. The precipitation height of the collected events ranged from 0.1 to 91 mm (Fig. 33a) for a total of 879 mm (vs. 1118 mm collected in 2006 and 881 mm in 2005).

The ranges of concentrations measured in these samples are indicated in Table 3. Concentrations (averaged over events) of Cl^-, SO_4^{2-} and K^+_ were smaller, of NO_3^-, Na^+, NH_4^+ and Ca^{2+} larger in 2007 compared to the 1990-1999 averages. The precipitation samples collected in 2007 were all acidic.

Table 3: parameters relative to the precipitation samples collected in 2007 (averages per rain event)

	pH	cond.	Cl^-	NO_3^-	SO_4^{2-}	Na^+	NH_4^+	K^+	Mg^{2+}	Ca^{2+}
		$\mu S\ cm^{-1}$	$mg\ l^{-1}$	$mg\ l^{-1}$	$mg\ l^{-1}$	$mg\ l^{-1}$	$mg\ l^{-1}$	$mg\ l^{-1}$	$mg\ l^{-1}$	$mg\ l^{-1}$
average	5.28	21.28	0.37	5.51	2.24	0.27	2.05	0.08	0.06	0.48
min	4.23	8.09	0.09	1.32	0.85	0.06	0.51	0.02	0.02	0.14
max	6.00	48.07	0.67	16.27	4.35	0.46	6.07	0.15	0.15	1.17
1990-1999	4.40	24.86	0.44	3.94	3.07	0.23	1.25	0.09	0.06	0.45

Wet deposition occurred rather evenly from mid February till mid December (Fig. 34), with only a few intense events. The annual wet deposition flux of the main acidifying and eutrophying species were 1.3, 2.5, and 1.1 g m^{-2} for SO_4^{2-}, NO_3^-, and NH_4^+, respectively. These fluxes were slightly smaller than in 2006 with values of 1.7, 3.1 and 1.3 g m^{-2} for the respective species.
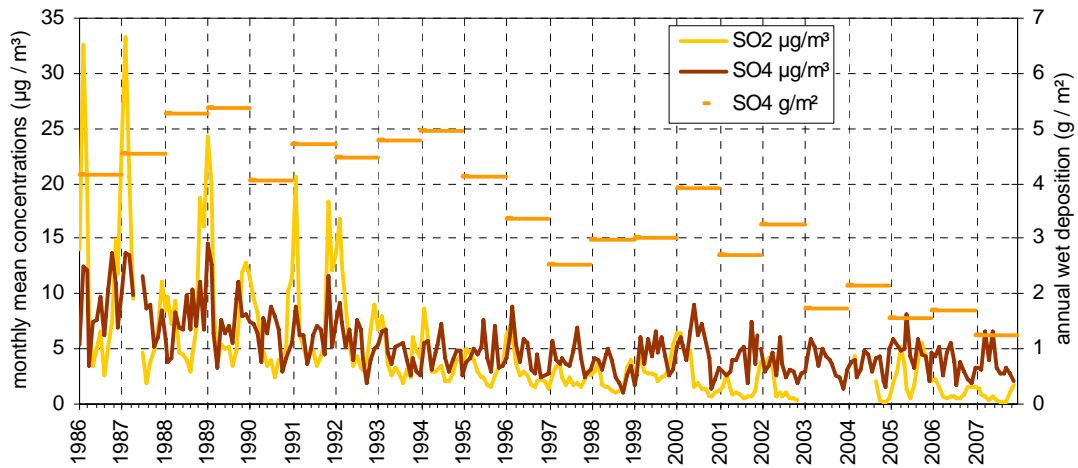
Fig. 35: oxidized sulfur species monthly mean concentrations and yearly wet deposition
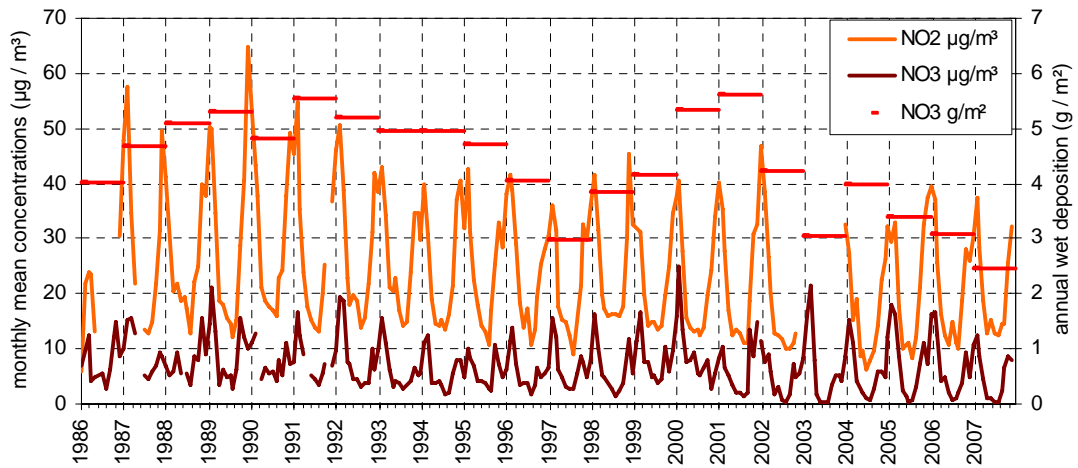

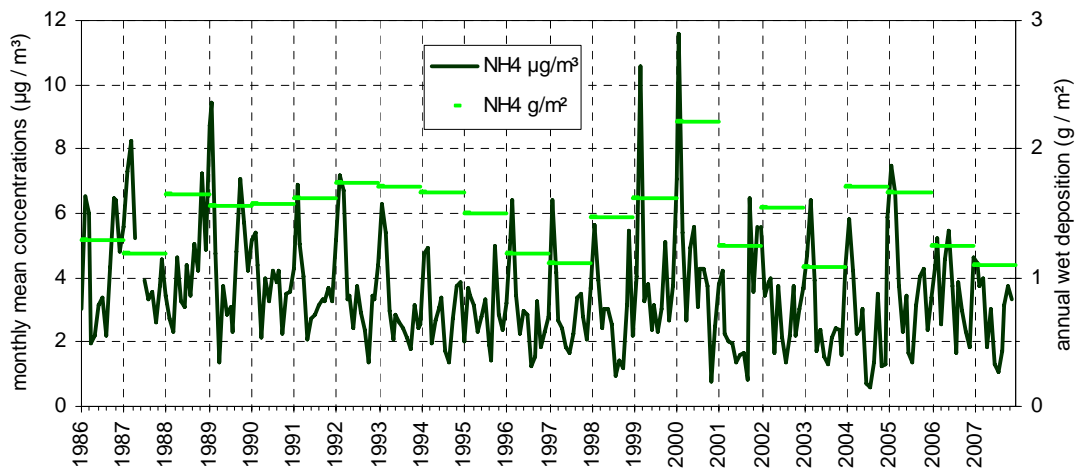*Fig. 36: oxidized nitrogen species monthly mean concentrations and yearly wet deposition*

Fig. 37: reduced nitrogen species monthly mean concentration and yearly wet deposition

48

Results of year 2007 in relation to 2 decades of monitoring activities

Sulfur and nitrogen compounds

Both winter maxima and summer minima monthly mean concentrations of sulfur dioxide (SO_2) decreased by a factor >5 over the past 20 years (Fig. 35). Particulate SO_4^{2-} showed also a clear decreasing trend from 1986 to 1998 (factor 3), but seems to stabilize around the mean value for the 90's since then. It should be kept in mind that SO_4^{2-} concentrations were measured in PM10 from 2002 onwards, whereas it was measured in TSP (Total Suspended Particulate) from 1986 to 2001. However, simultaneous sampling of PM10 and TSP over 14 months showed that SO_4^{2-} in PM10 is generally less than 5 % lower than in TSP. SO_4^{2-} wet deposition in 2007 marks a new historical minimum. These data show that locally produced SO_2 decreased much more than possibly long-range transported SO_4^{2-} over the past 20 years.

Monthly mean concentrations of nitrogen dioxide (NO_2) do not show such a pronounced decreasing trend over the last 2 decades (Fig. 36). Wintertime NO_2 maxima indeed remained quite constant over 1993-2002, and did not reflect the 30 % abatement in NO_x emissions over the 1992-2000 period (Perrino and Putaud, 2003). However, NO_2 concentrations observed in 2007 were among the lowest in the data series. Particulate NO_3^- annual mean concentration reached its minimum in 2002, but concentrations observed in 2003 - 2007 were comparable to values observed in the mid-90's, mainly due to higher wintertime values. It should be noted that since October 2000, NH_4 and NO_3^- have been measured mostly from quartz fibre filters, which are known to lose NH_4NO_3 at temperatures > 20 °C. This might contribute significantly to the fact that NO_3^- summertime minima are particularly low since 2001. In 2007 however, NH_4 and NO_3^- have been measured from cellulose fibre filters in summertime, thus avoiding this negative artefact. Furthermore, NO_3^- was measured from PM10 from 2002, and no more from TSP, as over the 1986 to 2001 period. However, simultaneous sampling of PM10 and TSP over 14 months showed that NO_3^- in PM10 is generally less than 5 % lower than in TSP, like SO_4^{2-}. NO_3^- wet deposition annual flux observed in 2007 set a new historical minimum as well.

Monthly mean concentrations of NH_4^+ in the particulate phase appear to decrease over 1986 – 2007 (Fig. 37), especially because summertime minima decreased. 2007 behaves slightly different in this respect as the summertime minima was comparably high. There is no clear trend regarding NH_4^+ wintertime maxima. On average, NH_4^+ can neutralize all of the acidity associated with NO_3^- and SO_4^{2-} in the particulate phase. NH_4^+ is also quite well correlated with $NO_3^- + SO_4^{2-}$ in rainwater. NH_4^+ wet deposition was among the lowest values in the dataset in 2007.
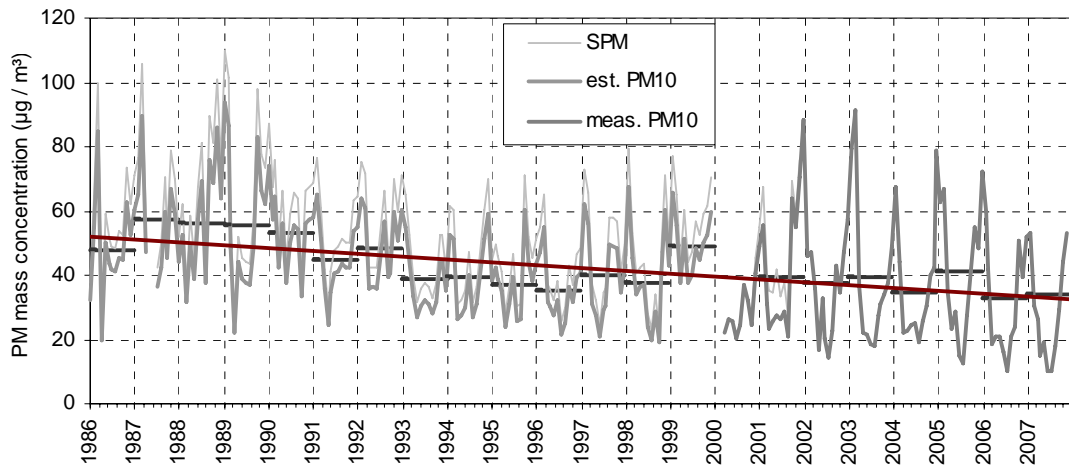
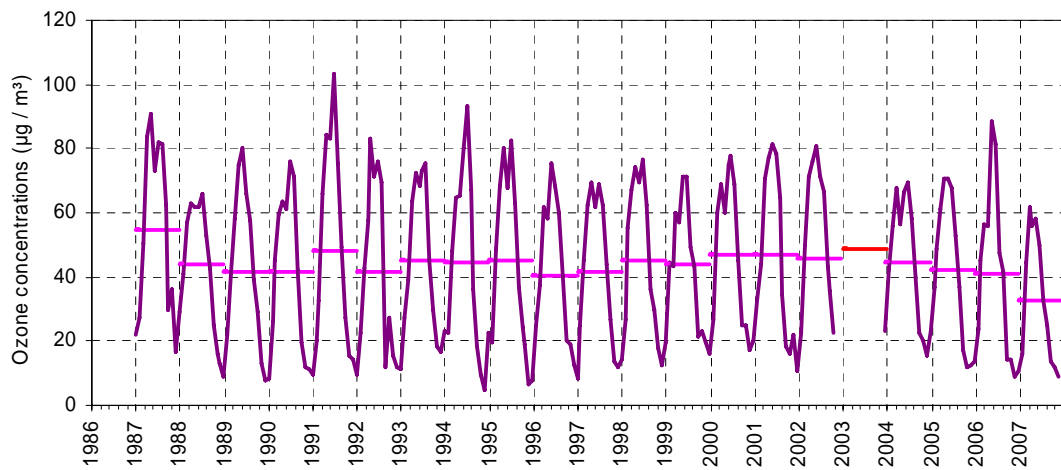*Fig. 38: particulate matter mass concentration monthly and annual averages*

Fig. 39: ozone yearly and monthly mean concentrations. 2003 data from Malpensa airport
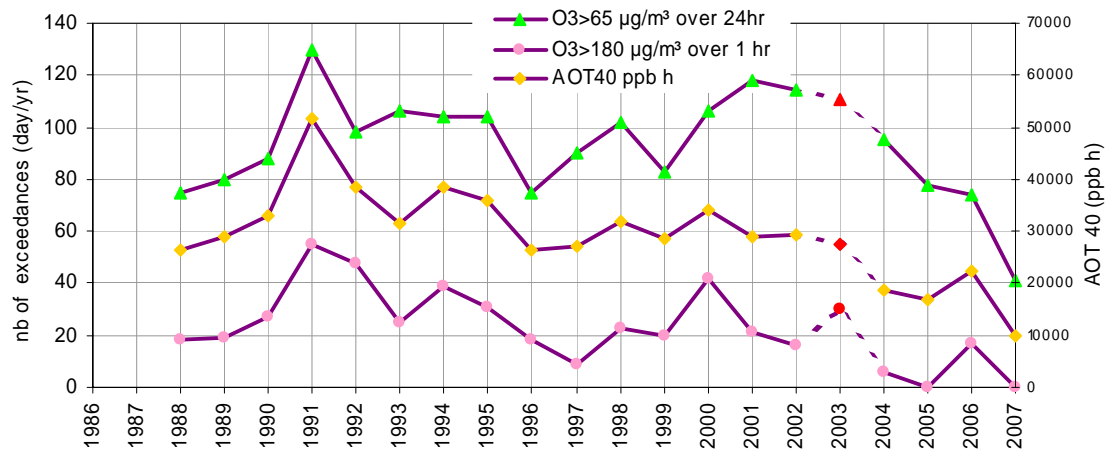

Fig. 40: AOT40 values and number of days on which indicated O3 limit values were reached. Red symbols indicate estimates based on Malpensa airport data (no data from Ispra in 2003)

Particulate matter mass

The PM10 values observed in 2007 agree with the general decreasing trend in PM10 observed over the last 2 decades (Fig. 38). In fact, in 2007 the average PM10 concentration reached a new historic minimum of 30 µg/m³. A linear fit indicates that PM10 has been decreasing by about 0.9 µg m^{-3} yr^{-1} during 1986-2007. It should be kept in mind that PM10 concentrations were estimated from TSP mass concentration measurements (carried out by weighing at 60 % RH and 20 °C cellulose acetate filters sampled without any particle size cut-off and "dried" at 60 °C before and after sampling) over 1986-2000, based on a comparison between TSP and PM10 over the Oct. 2000 - Dec. 2001 period (R^2 = 0.93, slope = 0.85).

Ozone

Fig. 39 shows monthly and yearly mean O_3 concentrations observed since 1987. To close the gap due to the data acquisition breakdown in 2003, O_3 data from Malpensa airport have been used to estimate values based on a comparison between Ispra and Malpensa during 2004. No clear trend in O_3 annual mean concentrations can be deduced from the observations over 1987-2007, although the winter lows and summer highs generally decrease since 2001. The annual average in 2007 is a new historic low, the summertime monthly maximum this year was the lowest one recorded as well. Also the wintertime minimum in 2007 was lower compared to the previous years.

Fig. 40 shows that AOT40, the vegetation exposure to above the O_3 threshold of 40 ppb (80 µg/m³) started to decrease again from 2002. This trend continued in 2007 with an all time low value of 9850 ppb h. Also the number of days with a mean O_3 concentration > 65 µg/m³ (vegetation protection limit) have a new historic minimum of 40 days. The number of days on which the limit value for public information (180 µg/m³ over 1hr) was reached or exceeded also generally decreased from 2000 (2003 and 2006 excepted). In 2007 this limit has not been reached at all.

Conclusion

Excluding CO, gas phase measurements were carried out throughout 2007 without major gaps. Aerosol sampling on quartz fibre filter (TISSUE QUARTZ 2500QAT-UP from PALL Life Sciences) for gravimetric and chemical analyses were also performed over the whole year. We collected PM2.5 daily and PM10 for a limited number of samples with a Partisol dichotomous sampler. Gravimetric analyses of PM2.5 at 20 % and 50 % RH correlated rather well with the FDMS-TEOM measurements of PM10. All PM2.5 samples were analyzed for carbonaceous components with the new Sunset Lab OC/EC instrument using the EUSAAR-2 protocol. The EMEP 2007 intercomparison for rainwater analyses suggests that we performed well with the analyses, the largest discrepancy of -8% was observed for SO_4. The ionic balance in both rainwater and aerosol samples demonstrate a perfect agreement between NH_4^+ measurement on the one hand, and NO_3^- + SO_4^{2-} measurements on the other hand. Particle number size distributions were performed with a DMPS and an APS along the year, except for maintenance periods. The average aerosol density of 1.2 g/cm^3, derived from the weighed mass and DMPS plus APS volume was still rather low, especially compared to the 2005 value of 1.5 g/cm^3. Comparison of the aerosol volume and mass concentrations with other variables (chemical mass, extinction) suggest that the aerosol volume was overestimated. Aerosol scattering and absorption coefficients were derived from Nephelometer and Aethalometer measurements, applying state-of-the-art corrections to these measurements. However, these data were not normalized to a standard relative humidity. The extinction-to-mass ratio of 4.5 $m^2\,g^{-1}$ measured in 2007 is comparable to 4.1 $m^2\,g^{-1}$ obtained in 2006. Both are consistent with the value that can be calculated from the mean PM2.5 chemical composition, which sums up to 4.7 $m^2\,g^{-1}$ in 2007.

The 2007 data listed by EMEP as core parameters have been reported to NILU (http://www.nilu.no/projects/ccc/).

Sulfur dioxide (SO_2) and nitrogen dioxide (NO_2) presented seasonal variations (low concentrations in summer, higher concentrations in winter) comparable to the other years, and consistent seasonal changes in pollutant dispersion. Rather low O_3 maximum concentrations were observed from May till August, in line with the seasonal variations in solar irradiation and quite high precipitations in June and August. The measurements in 2007 of the SO_2 concentrations and, to a lesser extend, of summertime NO_2 concentrations were in line with the long-term trends in SO_2, i.e. decreasing, and summertime NO_2, i.e. decreasing since 1998. The decreasing trend in O_3 extreme value frequency continued

in 2007 when exceedances of the 1hr O_3 limit value of 180 µg/m³ were not observed. Also the yearly average O_3 concentration marks a new historic minimum.

Gravimetric measurements operated at 20 % and 50 % RH confirmed that PM mass measured at 20 % RH was consistently ~5 % lower than PM mass measured at 50 % RH. The ratio between PM2.5 mass, measured at 50 % RH and PM10 mass, measured with the FDMS-TEOM, was 0.87 in 2007. The one obtained between weighing both PM2.5 and PM10 was 0.82, but it had limited statistics. The full chemical characterization of PM2.5 (main inorganic ions, organic carbon, black carbon and estimated mineral dust) showed that particulate organic matter (POM) is usually by far the main aerosol component. However, there is a clear enhancement of the secondary inorganic component contribution when shifting from cleaner (PM10 < 25 µg/m³) to more polluted periods (PM10 > 50 µg/m³). It should be noted that with the assumption used to estimate POM and dust from organic carbon (OC) and Ca^{2+}, respectively, the whole PM2.5 mass concentration could be explained rather well in 2007 except for a few periods in January and February. The PM10 mass annual average of 29.5 µg/m³ did not exceeded the EU limit value (40 µg/m³). The long term time series still suggests a PM10 mass concentration decrease of 0.9 µg m^{-3} yr^{-1} over the last 2 decades.

Average particle number was close to 9200 cm^{-3}. Particle number size distributions were generally slightly bimodal, with a submicron mode at ca. 100 nm (dry) and a less pronounced coarse mode around 2 µm. Atmospheric aerosol scattering and absorption coefficients at various wavelengths were derived from Nephelometer and Aethalometer measurements at not controlled (but generally lower than ambient) relative humidity. The mean single scattering albedo (at RH generally < 40 %) was 0.79 in 2007.

Aerosol backscatter and extinction profiles were obtained with a LIDAR during 2007. Within the EARLINET project, 44 % of the scheduled aerosol backscatter profiles could be submitted to the EARLINET database.

The aerosol extensive parameters measured at JRC-Ispra (at ground level) all follow a comparable seasonal trend with minima in winter. These parameters are generally well correlated and lead to reasonable degrees of chemical, physical, and optical closures.

The concentrations of some rainwater components (Cl$^-$, SO$_4^{2-}$ and K$^+$) were lower in 2007 compared to the 1990-1999 average, for others they were higher (NO$_3^-$, Na$^+$ and Ca^{2+}). The wet deposition fluxes of the main acidifying and eutrophying species showed for all but NH$_4$ new historic minima. No clear event of "desert dust wet deposition" was detected in 2007.

References

Anderson, T.L., and Ogren, J.A., Determining aerosol radiative properties using the TSI3563 integrating nephelometer, *Aerosol Sci. Technol.*, **29**, 57-69, 1998.

Arnott, W.P., Hamasha, K., Moosmüller, H., Sheridan, P.J., and Ogren, J.A., Towards aerosol light-absorption measurements with a 7-wavelength aethalometer, …, *Aerosol Sci. Technol.*, **39**, 17-29, 2005.

Burch, D. E.; Gates, F. J.; Pembrook, J. D., Ambient carbon monoxide monitor. Research Triangle Park, NC: U.S. Environmental Protection Agency, Environmental Sciences Research Laboratory; report no. EPA-600/2-76-210, 1976.

Cavalli, F., Putaud, J.P., Toward a standardized thermal-optical protocol for measuring atmospheric organic and elemental carbon: The EUSAAR protocol, *EUR* **23441** EN, 2008.

Cooke, W.F., Liousse, C., Cachier, H., and Feichter, J., Construction of a 1x1°fossil fuel emission data set for carbonaceous aerosol and implementation and radiative impact in the ECHAM4 model, *J Geophys. Res.*, **104**; 22,137-22,1999.

Hess, M., Koepke, P. Schult, I., Optical Properties of Aerosols and Clouds: The Software Package OPAC, *Bull. of Am. Meteorol. Soc.*, **79**; 831-844, 1998.

Kiehl, J. T., Schneider, T. L., Rasch, P. J., Barth, M. C., Wong, J., Radiative forcing due to sulfate aerosols from simulations with the National Center for Atmospheric Research Community Climate Model, Version 3 (Paper 1999JD900495), *J. Geophys. Res.,* **105**; 1441-1458, 2000.

Mira-Salama, D., Van Dingenen, R., Gruening, C., Putaud, J.-P, Cavalli, F., Cavalli, P., Erdmann, N., Dell'Acqua, A., Dos Santos, S., Hjorth, J., Raes, F., Jensen, N.R., Using Föhn conditions to characterize urban and regional sources of particles, *Atmospheric Research* **90**, 159–16, 2008.

Nessler, R., Weingartner, E., and Baltensperger, U., Adaptation of dry nephelometer measurementsto ambient conditions at the Jungfraujoch, *Environ. Sci. Technol.*, 39, 7, 2219-2228, 2005.

Perrino, C., and Putaud, J.P., Assessment of the EMEP measurement and modelling work in Europe from 1977 until Today: national contribution of Italy, *EUR* **20979** EN, 2003.

Schmid, O., et al., Spectral light absorption by ambient aerosols influenced by biomass burning in the Amazon Basin I: comparison and field calibration of absorption measurements techniques, *Atmos. Chem. Phys.*, **6**, 3443-3462, 2006.

Weingartner, E., Saathoff, H., Schnaiter, M., Streit, N., Bitnar, B., and Baltensperger, U., Absorption of light by soot particles: determination of the absorption coefficient by means of aethalometers, *J. Aerosol Sci.*, **34**, 1445-1463, 2003.

Weitkamp, C. (editor), LIDAR Range-Resolved Optical Remote Sensing of the Atmosphere, *Springer*, New York, 2005.

Abstract

The aim of the JRC-Ispra station for atmospheric research (45°49'N, 8°38'E) is to monitor atmospheric parameters (pollutant concentrations and fluxes, atmospheric particle chemical composition, number size distribution and optical properties) to contribute in assessing the impact of European policies on air pollution and climate change. The station has been operated continuously since November 1985, with a gap in gas phase data due to a severe breakdown of the data acquisition system in 2003 though.

The measurements performed in 2007 led to annual averages of ca. 32 µg m^{-3} O_3, 0.8 µg m^{-3} SO_2, 21 µg m^{-3} NO_2 and 30 µg m^{-3} PM10. Carbonaceous species (organic matter plus elemental carbon) are the main constituents of PM2.5 (> 55 %) followed by NH_4NO_3 (20-30 %) and $(NH_4)_2SO_4$ (10-20 %). The measurements confirmed the seasonal variations observed over the previous years, mainly driven by meteorology rather than by changes in emissions. Aerosol physical and optical properties were also measured in 2007. The average particle number (from 10 nm to 10 µm) was about 9200 cm^{-3} in 2007. The mean (close to dry) aerosol single scattering albedo (0.79) was low compared to the values generally observed in Europe, which means that the cooling effect of aerosols is reduced in our region compared to others.

Long-term trends (over 20 years) show consistent decreases in sulfur concentrations and deposition, PM mass concentration (-0.9 µg m^{-3} yr^{-1}) and in extreme ozone value occurrence frequency. The decreasing trends in oxidised and reduced nitrogen species are much less pronounced. However, historical minimum in NO_3^-, NH_4^+, (and SO_4^{2-}) wet deposition, as well as in O_3 pollution indicators (AOT40 and SOMO35) were observed in 2007.

The mission of the JRC is to provide customer-driven scientific and technical support for the conception, development, implementation and monitoring of EU policies. As a service of the European Commission, the JRC functions as a reference centre of science and technology for the Union. Close to the policy-making process, it serves the common interest of the Member States, while being independent of special interests, whether private or national.